

Latent space models for multiplex networks with shared structure

Peter W. MacDonald, Elizaveta Levina, and Ji Zhu

Department of Statistics, University of Michigan

December 22, 2024

Abstract

Latent space models are frequently used for modeling single-layer networks and include many popular special cases, such as the stochastic block model and the random dot product graph. However, they are not well-developed for more complex network structures, which are becoming increasingly common in practice. Here we propose a new latent space model for multiplex networks: multiple, heterogeneous networks observed on a shared node set. Multiplex networks can represent a network sample with shared node labels, a network evolving over time, or a network with multiple types of edges. The key feature of our model is that it learns from data how much of the network structure is shared between layers and pools information across layers as appropriate. We establish identifiability, develop a fitting procedure using convex optimization in combination with a nuclear norm penalty, and prove a guarantee of recovery for the latent positions as long as there is sufficient separation between the shared and the individual latent subspaces. We compare the model to competing methods in the literature on simulated networks and on a multiplex network describing the worldwide trade of agricultural products.

1 Introduction

Network data have become commonplace in many statistical applications, including neuroscience, social sciences, and computational biology, among others. In the vast majority of cases, these network data are represented as *graphs*. At a minimum, a graph $G = (V, E)$ has a node set V and an edge set E , with each edge connecting a pair of nodes, but frequently additional information is available, such as node attributes, edge weights, multiple types of edges, and so on. While a lot of work has been done on a single network with binary edges, as the complexity of network data structure increases, the availability of statistical methods and models dwindles rapidly. There is a strong need for rigorous statistical analysis to keep up with the rapidly increasing complexity of real datasets.

One such complex network data structure is the *multilayer graph* [Kivelä et al., 2014], a highly general mathematical object which can describe multiple graphs, dynamic graphs, hypergraphs, and vertex-colored or edge-colored graphs. In addition to a node set and an edge set, a multilayer graph includes a layer set L . A node may appear on any or all layers, and each edge connects two vertices, including the possibility of connection in the same layer (intra-layer edge), across layers (inter-layer edge), and between the same node on different layers. For example, a general multilayer network could be used to represent a multi-modal (bus, train, bicycle, etc.) urban transportation network,

where each layer corresponds to a different mode of transportation, and edges define connections between stations.

The focus of this paper is on multiplex graphs, a type of multigraphs where a common set of n nodes appears on every layer, and no inter-layer edges are allowed. For example, the brain connectivity networks of a sample of people, or a multi-commodity international trade network (cf. Section 6) could be represented as a multiplex network where each layer corresponds to a subject, or a commodity respectively.

For the single undirected graph G with $|V(G)| = n$, a common approach to modeling is to assume that there are n latent variables $\{X_i\}_{i=1}^n \subseteq \mathcal{X}$, one for each node. Typically one further assumes that X_i and X_j fully parameterize the distribution of the edge variable $E_{ij} = \mathbf{1}((i, j) \in E(G))$, and all the edge variables are mutually independent [Matias and Robin, 2014]. The latent positions themselves are sometimes treated as fixed and sometimes as independent random variables; in the latter case the above assumptions are conditional on $\{X_i\}_{i=1}^n$. These models are called *latent space* models, and intuitively the latent variable X_i represents the behavior of node i through its position in the latent space \mathcal{X} . Matias and Robin [2014] distinguish between two cases: a discrete latent space $\mathcal{X} = \{1, \dots, K\}$, so that each node is in one of K latent classes, and $\mathcal{X} = \mathbb{R}^d$, so that each node is represented by its coordinates in Euclidean space. The first case includes the ubiquitous *stochastic block model (SBM)* [Holland et al., 1983], and a well-studied example of the second case is the *random dot product graph (RDPG)* [Athreya et al., 2017, Young and Scheinerman, 2007]. Models in the seminal papers of Hoff et al. [2002] and Handcock et al. [2007] correspond to the second case as well.

Some of the frequentist approaches to latent space models treat the latent variables as random and focus on estimation of and inference for the parameters governing their distribution(s), for example Bickel et al. [2013] in the SBM setting. Many others do inference conditional on the latent variables and estimate them, especially when the goal is community detection, for example, Lei and Rinaldo [2015] in the SBM setting, Athreya et al. [2017] in the RDPG setting, and Ma et al. [2020] in a latent space model with edge covariates.

Some extensions of latent space models for multilayer networks have been proposed in the literature. This can be divided into two general categories: general multiple networks, for instance from repeated measurements or multiple subjects; and dynamic or time-varying networks, for which the layers have a natural ordering. A review paper [Kim et al., 2018] details recent developments in the dynamic setting.

In the multiple networks setting, latent space models with a Bayesian approach to estimation have been proposed by Gollini and Murphy [2016], Salter-Townshend and McCormick [2017], and D’Angelo et al. [2019], among others. These approaches tend to be computationally expensive. For larger networks we aim to work with, we will focus on three recent frequentist approaches to latent space and low-rank modeling for multiple networks, as baselines to contrast to our proposal in this paper. Arroyo et al. [2019] consider a collection of independent RDPGs with a common invariant subspace. That is, the expected adjacency matrices for each layer are assumed to share a common, low-dimensional column space. This is similar to approaches taken by Levin et al. [2017], Wang et al. [2019b], and Nielsen and Witten [2018]. However, they do not consider the case where each layer also contains meaningful individual signal in addition to shared structure.

Zhang et al. [2020] consider a model where expected adjacency matrices (after a logistic transformation) share common low-rank structure. This framework allows for layer-specific parameters controlling degree heterogeneity, but no other individual structure.

Wang et al. [2019a] aim to decompose each expected adjacency matrix into a common and individual

part after applying a logistic transformation. They assume that the individual part is low-rank, but make no such assumptions on the common part. Thus this method loses the interpretability afforded by the latent space approach, and has high variability unless there are a large number of layers.

In extending latent space models to the multiple networks setting, we seek a modeling approach which can leverage shared structure to improve estimation accuracy, but in an adaptive way, learning how much the layers have in common from the data instead of assuming that the entire latent representation is shared across all layers. We also allow for non-trivial individual structure in order to robustly estimate truly common structure.

As a motivating example, consider (as we will see in Section 6) a multiplex network of international trade, where nodes correspond to countries, layers to different commodities, and each (weighted) intra-layer edge is the total trade of a given agricultural commodity between two nations. We would expect the structure in this network to be governed by node attributes corresponding to, for instance, geographical region, language or climate. Some of these attributes would be expected to affect all commodities similarly; geographical proximity would encourage trade of any commodity. On the other hand, some of these attributes may differ across layers; climate may encourage production and thus trade of some commodities but not others, depending on what crops are easiest to grow in a given country's climate. In a setting like this, if latent space models were fit to each layer individually, (1) a fitting procedure cannot leverage the shared structure across layers, and (2) the latent representation of the common structure will not be automatically aligned across layers. On the other hand, if a single latent space model is fit to all network layers jointly, or to some aggregated version, (1) an influential individual latent dimension, or one that is shared by some but not all layers, may be erroneously identified as a common effect; or (2) the influence of a common latent dimension may be overstated if it is not orthogonal to the individual latent dimensions. The model we propose in the next section aims to address these shortcomings.

2 A new model for multiplex networks

Here we propose a new model for MULTIplex NETworks with Shared Structure (MultiNeSS) with the goal of ultimately learning the amount of shared structure from data. We start by fixing notation. Suppose that we observe m undirected networks, weighted or unweighted, on a common set of n nodes with no self loops. The networks are represented by their adjacency matrices $\{A_k\}_{k=1}^m$ where $A_k \in \mathbb{R}^{n \times n}$ for $k = 1, \dots, m$. Each node i is associated with a fixed latent position describing its function in layer k , denoted $x_{k,i} \in \mathbb{R}^d$. The edges are assumed independent conditional on these latent positions: for $i < j$ and $k = 1, \dots, m$,

$$A_{k,ij} \stackrel{\text{ind}}{\sim} Q(\cdot; \kappa(x_{k,i}, x_{k,j}), \phi),$$

where $Q(\cdot; \theta, \phi)$ is some edge entry distribution with a scalar parameter θ and possible nuisance parameters ϕ , and $\kappa(\cdot, \cdot)$ is a symmetric similarity function, implying that the parameter θ captures the effect of the latent similarity of nodes i and j in layer k on the corresponding edge. We denote the latent positions for layer k by $X_k \in \mathbb{R}^{n \times d}$, for $k = 1, \dots, m$, where the i th row of the $n \times d$ matrix X_k corresponds to the latent position of node i in layer k .

The choice of similarity function κ may affect identifiability of X_k . For instance, if $\kappa(x, y) = \psi(x^\top y)$ is an invertible scalar function ψ applied to the Euclidean inner product, each X_k is only identifiable up to a common orthogonal rotation of the rows. If $\kappa(x, y) = \psi(\|x - y\|_2)$ is similarly defined as an invertible function of the Euclidean distance rather than the Euclidean inner product, X_k is only identifiable up to a common orthogonal rotation of the rows and a common shift of each

row by a vector in \mathbb{R}^d .

The key assumption of the MultiNeSS model is that some, but not all, structure is shared across network layers. We suppose that the matrix X_k can be written as

$$X_k = \begin{bmatrix} V & U_k \end{bmatrix}, \quad (1)$$

where $V \in \mathbb{R}^{n \times d_1}$ gives a matrix of *common* latent position coordinates, and $U_k \in \mathbb{R}^{n \times d_2}$ are *individual* latent position coordinates for layer k . Writing X_k in this way further complicates identifiability. The model will certainly be identifiable only up to some invariant transformation of the rows of each U_k , and of V , but we would still want V to be identifiable in such a way that it is aligned across all the layers. Intuitively, for this to hold we need the common dimension d_1 to be maximal and unique, in the sense that any transformation which aligns the first d_1 coordinates must partition X_k into V and U_k as written above. We will formalize this intuition in Section 2.1. First, we present some concrete examples of latent space models which fit the general MultiNeSS model framework.

Example 1 (Low rank, Gaussian errors). As a simple example, let the similarity function κ be the Euclidean inner product, and $Q(\cdot; \theta, \sigma)$ is the Gaussian distribution $\mathcal{N}(\theta, \sigma^2)$. Then each layer's adjacency matrix has the expectation

$$\mathbb{E}A_k = VV^\top + U_k U_k^\top.$$

Each error matrix $E_k = A_k - \mathbb{E}A_k$ is symmetric with i.i.d. mean 0 Gaussian entries.

If the setting does not allow for self-loops, we can instead use $\mathbb{E}A_k = VV^\top + U_k U_k^\top - \text{diag}(VV^\top + U_k U_k^\top)$ to enforce zeros on the diagonal. The same can be done in any of the subsequent examples, if needed.

Example 2 (Low rank, exponential family errors). Let the similarity function κ be the Euclidean inner product again, and let $Q(\cdot; \theta)$ be a one-parameter exponential family distribution with natural parameter θ and log-partition function ν . That is,

$$Q(x; \theta) \propto \exp \{x\theta - \nu(\theta)\}.$$

For instance, Q may be a Bernoulli distribution, in which case

$$\nu(\theta) = \log(1 + e^\theta).$$

In the spirit of generalized linear models, we model the edges by applying the canonical link function $g = \nu'$ entry-wise, so that adjacency matrices now satisfy

$$\mathbb{E}A_{k,ij} = g(v_i^\top v_j + u_{k,i}^\top u_{k,j}),$$

for $k = 1, \dots, m$ and $1 \leq i, j \leq n$. In the Bernoulli example, the canonical link function is the inverse logistic function

$$g(\theta) = \frac{e^\theta}{1 + e^\theta}.$$

2.1 Identifiability

We present a sufficient condition for identifiability when κ is a scalar function of the inner product. For other choices of similarity function, conditions for identifiability will depend on the set of

invariant transformations which it induces.

For the inner product model with one layer, it is natural to assume that the matrix of latent positions $X \in \mathbb{R}^{n \times d}$ is full rank, that is, it has linearly independent columns. We show that a stronger linear independence condition for all pairwise concatenations of the latent position matrices is sufficient for identifiability in the proposed MultiNeSS model. The proof is given in Appendix B.1.

Proposition 1. Suppose $\kappa(x, y) = \psi(x^\top y)$ is an invertible scalar function of the inner product, the model is parameterized by V and $\{U_k\}_{k=1}^m$ as in (1), and for all $1 \leq k_1 < k_2 \leq m$, the $n \times (d_1 + 2d_2)$ matrix

$$\begin{bmatrix} V & U_{k_1} & U_{k_2} \end{bmatrix} \quad (2)$$

has linearly independent columns. Then the model is identifiable up to orthogonal rotation, that is, if the probability distributions induced by two different parametrizations (V, U_1, \dots, U_m) and (V', U'_1, \dots, U'_m) coincide, then

$$V = V'W_0, U_1 = U'_1W_1, \dots, U_m = U'_mW_m$$

for some orthogonal matrices $\{W_k\}_{k=0}^m$.

Similar identifiability conditions can be derived for different similarity functions κ , with the condition depending on the group of invariant transformations for κ . Note that Proposition 1 does not require the orthogonality of the columns of V and $\{U_k\}_{k=1}^m$, although clearly it will be satisfied if the columns are all mutually orthogonal.

We also note that the condition (2) can be relaxed, since we do not utilize the linear independence of all such matrices in the proof, which only requires (2) to hold for the pairs $\{1, 2\}, \{2, 3\}, \dots, \{m-1, m\}$. For an even weaker condition, suppose we construct an undirected graph \mathcal{G}_I on the network layers, with vertex set $\{1, \dots, m\}$, and edges defined by

$$k \sim l \iff \begin{bmatrix} V & U_k & U_l \end{bmatrix} \text{ is linearly independent.}$$

The argument used to prove Proposition 1 implies that the common latent dimensions can be uniquely identified on every connected component of \mathcal{G}_I . Thus, identifiability will hold as long as \mathcal{G}_I is connected. We also note that the same conditions and proof imply identifiability even if the individual latent position matrices have different column dimensions for different layers.

As a visual intuition, consider a simple case with $n = 10$, $d_1 = d_2 = 1$, $m = 2$. Standard results for the RDPG [Athreya et al., 2017] would suggest that the (2-dimensional) latent positions for each layer are only identifiable up to orthogonal rotations, which differ across layers. The recovered latent positions for the two layers may have different rotations, and thus would not share a common column according to the MultiNeSS model (1). Proposition 1 states that pairwise linear independence is sufficient to uniquely align the rotations, and identify the common and individual latent positions (up to sign).

In Figure 1 panels (A) and (B), we plot latent positions $\{(v_i, u_{k,i})\}_{i=1}^n$ in \mathbb{R}^2 for $k = 1$ and 2 respectively. The common dimension is on the x -axis and the individual dimension on the y -axis, thus the x -coordinates are constant in panels (A) and (B). In Figure 1 panels (C) and (D), we apply an orthogonal transformation to each of the latent positions, equivalent to applying an unknown (2-dimensional) orthogonal rotation. The dashed lines denote the original x -axis in the two rotated spaces; note that the coordinates of projection onto these directions are constant in the two panels. By Proposition 1, as long as (2) holds, the original x -axis is the unique direction with this property, and the coordinates of projection uniquely identify the entries of v (up to sign).

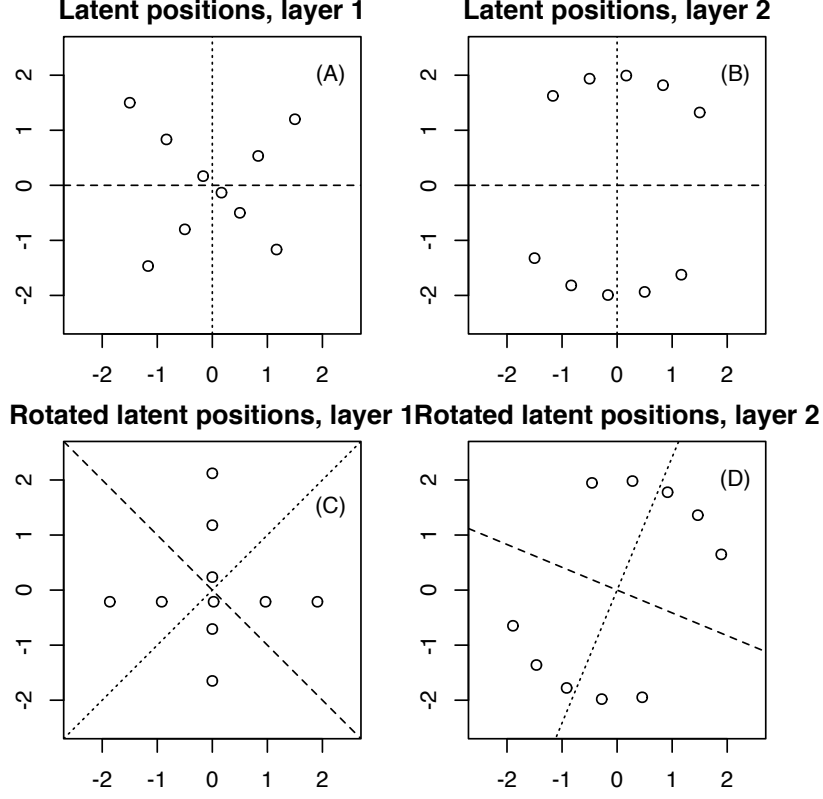


Figure 1: Latent positions before (top row) and after (bottom row) orthogonal rotation.

3 Fitting the MultiNeSS model

A natural approach to latent space estimation is likelihood maximization. A convex relaxation of the likelihood can be maximized by introducing a nuclear norm penalty, and by optimizing over the entries of the low-rank matrices $F = VV^\top$ and $G_k = U_k U_k^\top$ rather than the latent position matrices themselves.

3.1 Convex objective function

With the notation defined in Section 2, suppose κ is the Euclidean inner product in \mathbb{R}^d . In terms of the latent position parameters $(V, \{U_k\}_{k=1}^m)$, the negative log-likelihood takes the form (after dropping constants)

$$\ell(V, \{U_k\} | \{A_k\}) \propto - \sum_{k=1}^m \sum_{i,j} \log Q(A_{k,ij}; v_i^\top v_j + u_{k,i}^\top u_{k,j}, \phi), \quad (3)$$

where Q is the density of the edge weight distribution. Up to a rotation, we can rewrite this likelihood in terms of $F = VV^\top$ and $G_k = U_k U_k^\top$, and equivalently minimize

$$\ell(F, \{G_k\} | \{A_k\}) = - \sum_{k=1}^m \sum_{i,j} \log Q(A_{k,ij}; F_{ij} + G_{k,ij}, \phi)$$

subject to the constraints

$$\text{rank}(F) \leq d_1, \text{rank}(G_k) \leq d_2, F \in \mathbb{S}_+^n, G_k \in \mathbb{S}_+^n,$$

where \mathbb{S}_+^n is the positive-semidefinite cone of $n \times n$ matrices. To make this problem tractable, we drop the positive semi-definite constraint and perform a convex relaxation of the rank constraint, leading to the unconstrained convex optimization problem

$$\min_{F, G_k} \left\{ \ell(F, \{G_k\} | \{A_k\}) + \lambda \alpha \|F\|_* + \lambda \sum_{k=1}^m \|G_k\|_* \right\}, \quad (4)$$

where $\lambda \geq 0$ and $\alpha \geq 0$ are tuning parameters, and $\|\cdot\|_*$ denotes the nuclear norm of a matrix, equal to the sum of the singular values. Since the nuclear norm is convex, it is easy to see that (4) defines a convex optimization problem as long as the edge distribution Q is log-concave in θ . Even though we do not enforce the positive semi-definite constraint, we will show in Theorem 1 that when F and G_k contain sufficient signal, the solutions will be positive semi-definite with high probability.

3.2 Proximal gradient descent algorithm

The optimization problem can be solved by applying proximal gradient descent block-wise to each of the matrix arguments. In particular, we split the optimization variables into $m + 1$ blocks of n^2 variables: one block containing the entries of F ; and m blocks, one for the entries of each G_k for $k = 1, \dots, m$.

Then for each block, the negative log-likelihood is convex and differentiable, and the nuclear norm penalty term is convex and although non-differentiable, it has a well-defined proximal mapping for step size $\eta > 0$ [Fithian and Mazumder, 2018]. In particular, the nuclear norm scaled by $\lambda \geq 0$ has the proximal mapping

$$\text{argmin}_{M'} \frac{1}{2\eta} \|M - M'\|_F^2 + \lambda \|M\|_* = S_{\eta\lambda}(M),$$

where $\|\cdot\|_F$ denotes the matrix Frobenius norm, the Euclidean norm of the vectorized entries; and $S_T(\cdot)$ is the soft singular value thresholding operator with threshold $T \geq 0$. That is, for a diagonal matrix $M \in \mathbb{R}^{q \times q}$,

$$S_T(M) = \text{diag}((M_{11} - T)_+, \dots, (M_{qq} - T)_+),$$

and otherwise $S_T(M) = US_T(D)V^\top$, where $M = UDV^\top$ is the singular value decomposition (SVD) of M [Fithian and Mazumder, 2018]. Thus, we derive the following proximal gradient descent steps with step size η/m for updates of F , and η for updates of G_k , $k = 1, \dots, m$: at iteration step $t \geq 1$,

$$\hat{F}^{(t)} = S_{\eta\lambda\alpha/m} \left(\hat{F}^{(t-1)} + \frac{\eta}{m} \frac{\partial}{\partial F} \ell(\hat{F}^{(t-1)}, \{\hat{G}_{k'}^{(t-1)}\}) \right), \quad (5)$$

$$\hat{G}_k^{(t)} = S_{\eta\lambda} \left(\hat{G}_k^{(t-1)} + \eta \frac{\partial}{\partial G_k} \ell(\hat{F}^{(t)}, \{\hat{G}_{k'}^{(t-1)}\}) \right), \quad (6)$$

for $k = 1, \dots, m$.

When Q is a one-parameter exponential family, and the edge distribution is modeled through the canonical link function (see Example 2), the gradients take on a particularly nice form.

In particular, up to an additive constant, we have for fixed $k \in \{1, \dots, m\}$ and $1 \leq i, j \leq n$,

$$(\log Q)'(A_{k,ij}; F_{ij} + G_{k,ij}) = A_{k,ij} - \nu'(F_{ij} + G_{k,ij}) = A_{k,ij} - \mathbb{E}[A_{k,ij}; F_{ij} + G_{k,ij}],$$

where the final equality follows by the choice of link function $g = \nu'$. Thus the gradients with respect to each G_k can be interpreted as the residual from estimating the adjacency matrix by its expectation given the current low-rank parameters. The gradient with respect to F is the sum of the residuals over all the layers.

If $Q(\cdot; \theta, \phi)$ is the Gaussian distribution, as in Example 1, the appropriate link function is the identity link. Then with step size $\eta = 1$, proximal gradient descent recovers a natural alternating soft-thresholding algorithm: at iteration step $t \geq 1$,

$$\hat{F}^{(t)} = S_{\lambda\alpha/m} \left(\frac{1}{m} \sum_{k=1}^m (A_k - \hat{G}_k^{(t-1)}) \right), \quad (7)$$

$$\hat{G}_k^{(t)} = S_\lambda \left(A_k - \hat{F}^{(t)} \right), \quad (8)$$

for $k = 1, \dots, m$. In Section 4, we will provide theoretical guarantees on estimators found with this special case of proximal gradient descent. When the observed networks have no self-loops, we will perform proximal gradient steps which ignore the diagonal entries, which should provide better empirical results in this case.

The most computationally expensive part of each update step is the singular value decomposition (SVD) needed for soft singular value thresholding. If the full SVD is calculated, each iteration step has computational complexity of order $O(mn^3)$. In practice, we use a truncated SVD which only finds the first $s \ll n$ singular vectors and values, as in Wu et al. [2017], reducing complexity to $O(mn^2s)$.

3.3 Refitting step

As we will show in Theorem 1, recovery of the correct rank requires a tuning parameter of order $\lambda \sim \sqrt{n}$, and thus the effect of the soft thresholding step on the estimated eigenvalues will not disappear as $n \rightarrow \infty$.

As in Mazumder et al. [2010], we propose a refitting step after solving the convex problem, where we fix the ranks and eigenvectors of \hat{F} and \hat{G}_k for $k = 1, \dots, m$, and refit their eigenvalues to maximize the likelihood.

Based on the output from the first step, we write the eigen-decompositions

$$\begin{aligned} \hat{F} &= \tilde{V} \Lambda_V \tilde{V}^\top, \\ \hat{G}_k &= \tilde{U}_k \Lambda_{U,k} \tilde{U}_k^\top. \end{aligned}$$

Note that element-wise, we have

$$\hat{F}_{ij} = \sum_{\ell=1}^{\hat{d}_1} \lambda_{V,\ell} \tilde{V}_{i\ell} \tilde{V}_{j\ell},$$

where \hat{d}_1 is the rank of \hat{F} . For $k = 1, \dots, m$, the elements of \hat{G}_k can be expressed similarly, with

$\hat{d}_{k,2}$ denoting the rank of \hat{G}_k . Then, fixing \tilde{V} and \tilde{U}_k , the refitting step solves the convex problem

$$\min_{\Lambda_V, \Lambda_{U,k}} \left\{ - \sum_{k=1}^m \sum_{i,j} \log Q \left(A_{k,ij}; \sum_{\ell=1}^{\hat{d}_1} \Lambda_{V,\ell} \tilde{V}_{i\ell} \tilde{V}_{j\ell} + \sum_{\ell'=1}^{\hat{d}_{k,2}} \Lambda_{U,k,\ell'} \tilde{U}_{k,i\ell'} \tilde{U}_{k,j\ell'}, \phi \right) \right\}. \quad (9)$$

When Q is a one-parameter exponential family and the edge distribution is modeled through the corresponding canonical link function (see Example 2), this reduces to fitting a generalized linear model with responses $\{A_{k,ij}\}$, coefficients

$$\beta = \begin{bmatrix} \Lambda_{V,1} & \cdots & \Lambda_{V,\hat{d}_1} & \Lambda_{U,1,1} & \cdots & \Lambda_{U,m,\hat{d}_{m,2}} \end{bmatrix}^\top,$$

and predictors

$$X_{k,ij} = \begin{bmatrix} \tilde{V}_{i1} \tilde{V}_{j1} & \cdots & \tilde{V}_{i\hat{d}_1} \tilde{V}_{j\hat{d}_1} & 0 & \cdots & 0 & \tilde{U}_{k,i1} \tilde{U}_{k,j1} & \cdots & \tilde{U}_{k,i\hat{d}_{k,2}} \tilde{U}_{k,j\hat{d}_{k,2}} & 0 & \cdots & 0 \end{bmatrix}^\top.$$

With the solution to the refitting step problem (9), we can construct the final estimates for the low-rank matrices,

$$\begin{aligned} \check{F} &= \tilde{V} \hat{\Lambda}_V \tilde{V}^\top, \\ \check{G}_k &= \tilde{U}_k \hat{\Lambda}_{U,k} \tilde{U}_k^\top. \end{aligned}$$

3.4 Choosing tuning parameters

A standard method for choosing tuning parameters is cross-validation, which requires some care on networks. We take an approach motivated by the edge cross-validation for networks [Li et al., 2020], where a random subsample of node pairs is repeatedly removed, a low-rank matrix completion method is applied to the adjacency matrix to impute the missing pairs, and the original method is refit on the completed matrix. Tuning parameters are then selected to minimize a loss function evaluated on the held-out edges.

While the general edge cross-validation procedure [Li et al., 2020] contains an imputation step followed by a fitting step, our convex fitting approach can be applied directly to adjacency matrices with missing entries. Suppose we subsampled matrices $\{A_k\}_{k=1}^m$ by removing the values for a random sample of indices (i, j, k) (accounting for symmetry). Denote the set of remaining indices by Ω . The new log-likelihood will resemble (3), but with the summation restricted to the triples in Ω , and the same proximal gradient descent algorithm can be applied.

Similar to the approach taken by Lock et al. [2020] for low-rank multiview data matrices, the tuning parameters can also be chosen adaptively using random matrix theory. In particular, in Example 1 with known σ , bounds on the singular values of random matrices would suggest setting

$$\lambda = (2 + \delta) \sigma \sqrt{n}$$

for a constant δ . Gavish and Donoho [2014] introduce an estimator $\hat{\sigma}_{\text{MAD}}$ for σ based on the median singular value and suggest setting $\delta \doteq 0.309$, which is optimal for hard singular-value thresholding. However, δ could also be selected using edge cross-validation. Further, since we assume the layers are independent, bounds on the sum of the layer-wise error matrices $\sum_k E_k$ would suggest setting $\alpha = \sqrt{m}$. This adaptive tuning scheme is used for the convex estimation approaches in Section 5. While this approach is designed with Example 1 in mind, it gives sensible results in Example 2 with

Bernoulli edges as well.

This adaptive tuning approach can also be used to account for layer-specific variances, with an alternative nuclear norm penalty

$$\alpha \left(\frac{1}{m} \sum_{k=1}^m \lambda_k^2 \right)^{1/2} \|F\|_* + \sum_{k=1}^m \lambda_k \|G_k\|_*,$$

which allows for layer-specific tuning parameters λ_k . As above, we choose $\alpha = \sqrt{m}$, and

$$\lambda_k = (2 + \delta) \hat{\sigma}_{\text{MAD}}^2(A_k) \sqrt{n}, \quad (10)$$

for $k = 1, \dots, m$. Here, $\hat{\sigma}_{\text{MAD}}^2(A_k)$ estimates the entry-wise variance for layer k , and δ is a constant which is either chosen a priori or selected using edge cross-validation. This layer-specific adaptive tuning is used for the real data analysis in Section 6.

4 Theoretical guarantees

4.1 Notation

We denote the matrix ℓ_2 operator norm by $\|M\|_2$. Let

$$[M]_d = \operatorname{argmin}_{M': \operatorname{rank}(M') \leq d} \|M - M'\|_F,$$

which is well-defined by the Eckart-Young Theorem as the truncation of the SVD of M to the largest d singular values. Let \mathcal{O}_d denote the set of $d \times d$ rotation (orthonormal) matrices. Let $\operatorname{col}(M)$ and $\operatorname{row}(M)$ denote the column and row spaces of a matrix M , respectively. For a symmetric matrix M , let $\gamma_i(M)$ denote the i th eigenvalue of M , with eigenvalues ordered from largest to smallest in magnitude.

4.2 Main results

Throughout this section we assume the model described in Example 1, where $Q(\cdot; \theta, \sigma)$ is the Gaussian distribution with known variance σ^2 . We allow the dimensions n, m, d_1 and d_2 to grow, subject to the following restrictions:

Assumption 1.

$$\begin{aligned} d_2 2^{d_2} m^2 n^{1-2\tau} &= o(1), \\ d_1 m^{-1} &= o(1), \\ d_2 m^{-1} &= o(1), \end{aligned} \quad (11)$$

for some constant $\tau \in (1/2, 1]$.

We study the estimator of the MultiNeSS model, defined as the limit of the proximal gradient update steps (7) and (8), starting from some initial value $\hat{F}^{(0)}$. Let \hat{F} and $\{\hat{G}_k\}_{k=1}^m$ denote the limits of this proximal gradient descent algorithm as $t \rightarrow \infty$.

For $k = 1, \dots, m$, let

$$G_k = \bar{U}_k \Gamma_k \bar{U}_k$$

denote the eigen-decomposition of each G_k , and

$$F = \bar{V} \Gamma_F \bar{V}^\top$$

denote the eigen-decomposition of F . Suppose that they satisfy the following assumptions.

Assumption 2.

$$b_1 n^\tau \leq \gamma_{d_2}(G_k) \leq \gamma_1(G_k) = \|G_k\|_2 \leq B_1 n^\tau, \quad (12)$$

$$b_1 n^\tau \leq \gamma_{d_1}(F) \leq \gamma_1(F) = \|F\|_2 \leq B_1 n^\tau. \quad (13)$$

for all $k = 1, \dots, m$, and uniform constants $0 < b_1 \leq B_1$.

Further, assume

$$\|\bar{V}^\top \bar{U}_k\|_2 = o(d_1^{-1/2} m^{1/2} n^{1/2-\tau}), \quad (14)$$

and

$$\|\bar{U}_{\mathcal{A}}^\top \bar{U}_k\|_2 \leq B_2 \sigma |\mathcal{A}|^{1/2} n^{1/2-\tau} \quad (15)$$

for some uniform constant $B_2 > 0$, where $\mathcal{A} \subseteq \{1, \dots, m\} \setminus \{k\}$, and $\bar{U}_{\mathcal{A}}$ is an orthonormal basis for $\sum_{j \in \mathcal{A}} \text{col}(G_j)$.

In particular, for $k_1 \neq k_2$,

$$\|\bar{U}_{k_1}^\top \bar{U}_{k_2}\|_2 \leq B_2 \sigma n^{1/2-\tau}. \quad (16)$$

Note that (14), (15) and (16), although stated with fixed orthonormal bases, are basis-free, and can be written in terms of the maximal cosine similarity between elements of the two column spaces. That is, if S_1 and S_2 are two subspaces of \mathbb{R}^n , then for any of their respective orthonormal bases U_{S_1} and U_{S_2} ,

$$\|U_{S_1}^\top U_{S_2}\|_2 = \sup_{x \in S_1, y \in S_2} \frac{|x^\top y|}{\|x\|_2 \|y\|_2}.$$

Comparing (14) and (16), note that these conditions allow for slightly more similarity between the column spaces of F and any one G_k than between the column spaces of G_k and G_j for $k \neq j$.

With these assumptions we have the following consistency result. The proof is given in Appendix B.2.

Theorem 1. Suppose $Q(\cdot; \theta, \sigma) = \mathcal{N}(\theta, \sigma^2)$, and Assumptions 1 and 2 hold. Let $\lambda = 3\sigma\sqrt{n}$, and $\alpha = c_\alpha\sqrt{m}$, where c_α is a universal constant. Then with probability greater than $1 - (m+1)ne^{-C_0 n}$ for some universal constant $C_0 > 0$, the initializer

$$\hat{F}^{(0)} = \left[\frac{1}{m} \sum_{k=1}^m A_k \right]_{d_1}$$

satisfies

$$\|\hat{F}^{(0)} - F\|_F = o(n^{1/2}), \quad (17)$$

and for n sufficiently large, and all $k \in \{1, \dots, m\}$, we have

$$\begin{aligned}\frac{1}{n}\|\hat{F} - F\|_F &\leq C_1\sigma\sqrt{\frac{d_1}{mn}}, \\ \frac{1}{n}\|\hat{G}_k - G_k\|_F &\leq C_2\sigma\sqrt{\frac{d_2}{n}},\end{aligned}\tag{18}$$

for positive constants C_1 and C_2 which do not depend on n, m, d_1, d_2 , and σ . Moreover, \hat{F} and \hat{G}_k are positive semi-definite.

Remark 1. The initializer $\hat{F}^{(0)}$ uses the true value of d_1 , which is generally unknown in practice. However, since the objective is convex, the estimators should not be sensitive to the initial value.

Remark 2. The conditions of Theorem 1 provide a regime under which our convex approach achieves the same rate as an oracle hard thresholding approach. In particular, if we estimated G_k with full knowledge of F by

$$\hat{G}_k^{(\text{oracle})} = [A_k - F]_{d_2},$$

and F with full knowledge of G_k for $k = 1, \dots, m$, by

$$\hat{F}^{(\text{oracle})} = \left[\frac{1}{m} \sum_{k=1}^m (A_k - G_k) \right]_{d_1},$$

they would have the same Frobenius norm error rates as the estimators in Theorem 1.

Remark 3. In the proof of Theorem 1, we will bound the operator norms of the error matrices E_k for $k = 1, \dots, m$ using a concentration inequality for Gaussian random matrices [Bandeira and Van Handel, 2016]. With a different operator norm concentration inequality [Chatterjee, 2015], we can show that a similar result holds if the entries of E_k are uniformly bounded instead of Gaussian. For instance, this would provide consistency for an RDPG-like binary edge model with $F + G_k \in [0, 1]^{n \times n}$ for $k = 1, \dots, m$, and

$$A_{k,ij} \sim \text{Bernoulli}(F_{ij} + G_{k,ij})$$

for $i < j$ and $k = 1, \dots, m$.

While Assumption 1 allows us to match the oracle error rate, it also places a strong requirement on the latent dimensions, especially the individual latent dimension d_2 . Theorem 2 gives an alternative result under a weaker assumption on d_2 , when it is allowed to grow polynomially in n . The proof is given in Appendix B.3.

Assumption 3.

$$\begin{aligned}m^2 n^{1-2\tau} &= o(1), \\ d_2 d_1 m^{-1} &= o(1),\end{aligned}\tag{19}$$

for some constant $\tau \in (1/2, 1]$.

Theorem 2. Suppose $Q(\cdot; \theta, \sigma) = \mathcal{N}(\theta, \sigma^2)$, and Assumptions 2 and 3 hold. Let $\lambda = 3\sigma\sqrt{n}$, and $\alpha = c_\alpha\sqrt{d_2 m}$, where c_α is a universal constant. Then with probability greater than $1 - (m + 1)ne^{-C_0 n}$ for some constant $C_0 > 0$, the initializer

$$\hat{F}^{(0)} = \left[\frac{1}{m} \sum_{k=1}^m A_k \right]_{d_1}$$

satisfies

$$\|\hat{F}^{(0)} - F\|_F = o(n^{1/2}),$$

and for n sufficiently large, and all $k \in \{1, \dots, m\}$, we have

$$\begin{aligned} \frac{1}{n} \|\hat{F} - F\|_F &\leq C_3 \sigma \sqrt{\frac{d_1 d_2}{mn}}, \\ \frac{1}{n} \|\hat{G}_k - G_k\|_F &\leq C_4 \sigma \sqrt{\frac{d_2}{n}}, \end{aligned}$$

for positive constants C_3 and C_4 which do not depend on n, m, d_1, d_2 , and σ . Moreover, \hat{F} and \hat{G}_k are positive semi-definite.

Theorems 1 and 2 provide bounds on the recovery of the $n \times n$ matrix-valued parameters F and G_k for $k = 1, \dots, m$, however in practice we are often interested in the latent position matrices V and U_k as well. With an additional assumption on the eigenvalue gaps of F and G_k , the following Proposition 2 establishes overall consistency for an adjacency spectral embedding-based estimate of the latent positions, after suitable rotation.

Assumption 4.

$$\min_{j \in \{2, \dots, d_1\}} |\gamma_j(F) - \gamma_{j-1}(F)| \geq b_3 n^\xi \quad (20)$$

for some $\xi \in (1/2, \tau]$ and positive constant b_3 , and an analogous condition holds for the eigenvalues of each G_k matrix.

Then we have the following consistency result for the latent matrices V and U_k , up to rotation.

Proposition 2. Suppose the assumptions of Theorem 1 and Assumption 4 hold. Then with probability greater than $1 - (m+1)ne^{-C_0 n}$ for some universal constant $C_0 > 0$, and for sufficiently large n , \hat{F} and \hat{G}_k are positive-semidefinite, low-rank matrices for $k = 1, \dots, m$. Further, let \hat{V} be the $n \times d_1$ dimensional adjacency spectral embedding (ASE) of \hat{F} , and \hat{U}_k be the $n \times d_2$ dimensional ASE of \hat{G}_k for $k = 1, \dots, m$. Then we have

$$\frac{1}{\sqrt{d_1 n}} \inf_{O \in \mathcal{O}_{d_1}} \|\hat{V} - VO\|_F \leq C_5 \sigma d_1^{1/2} m^{-1/2} n^{\tau/2-\xi}, \quad (21)$$

$$\frac{1}{\sqrt{d_2 n}} \inf_{O \in \mathcal{O}_{d_2}} \|\hat{U}_k - U_k O\|_F \leq C_6 \sigma d_2^{1/2} n^{\tau/2-\xi}, \quad (22)$$

for $k = 1, \dots, m$ and for some positive constants C_5 and C_6 .

Remark 4. Since we assume $\xi > 1/2 \geq \tau/2$, Proposition 2 shows that under the asymptotic regime of Assumption 1, the average entry-wise error of the latent position matrices (after suitable rotation) goes to zero. As in Theorem 1, the rate of convergence for the common structure exceeds that of the individual structure by a factor of \sqrt{m} .

5 Evaluation on synthetic networks

5.1 Baseline methods

Throughout this section we compare the estimator for the MultiNeSS model to other baseline methods on two types of synthetic networks: with weighted edges generated according to the Gaussian

model in Example 1, and with binary edges generated according to the logistic model in Example 2. We compare to non-adaptive optimization approaches for the MultiNeSS model, and to other methods in the literature [Arroyo et al., 2019, Wang et al., 2019a] for multiple networks which can capture the common and/or individual low-rank structure.

We also include two non-convex oracle approaches. For the Gaussian model, we apply non-convex alternating rank truncation algorithm (denoted below by SVD) which assumes oracle knowledge of the true ranks d_1 and d_2 . The alternating updates for $t \geq 1$ are given by

$$\begin{aligned}\hat{F}_k^{(t)} &= \left[\frac{1}{m} \sum_{k=1}^m \left(A_k - \hat{G}_k^{(t-1)} \right) \right]_{d_1}, \\ \hat{G}_k^{(t)} &= \left[A_k - \hat{F}_k^{(t)} \right]_{d_2}\end{aligned}$$

and initialized with $\hat{G}_k^{(0)} = 0$ for $k = 1, \dots, m$. These update steps are applied until convergence, or until a pre-specified maximum iteration number t_{\max} is reached.

For the logistic model we compare our convex approach with a non-convex gradient descent algorithm, similar to Ma et al. [2020], which also assumes known d_1 and d_2 . This approach directly updates the entries of the latent position matrices V and $\{U_k\}_{k=1}^m$ by performing gradient descent on the negative log-likelihood function.

The recently proposed COSIE method [Arroyo et al., 2019] fits a low-rank model to multiple binary undirected networks on a common node set. COSIE provides estimates of the expected adjacency matrices for each layer, but does not decompose the estimate into common and individual parts, so we can only compare the accuracy of overall expectation. While COSIE is designed for the RDPG model, it can also be applied unchanged to the Gaussian model. We apply an oracle version of COSIE assuming knowledge of the true d_1 and d_2 . For a fair comparison to our method, we first identify the $d_1 + d_2$ leading eigenvectors for each layer, then use COSIE to fit a common invariant subspace of dimension $d_1 + m \cdot d_2$, the total number of latent dimensions in the MultiNeSS model.

The second baseline comparison is to the M-GRAF algorithm proposed by Wang et al. [2019a], for a similar logistic link model for multilayer networks with common and individual parts. The M-GRAF model does not assume any structure, low-rank or otherwise, for entries of the common matrix F and does not employ regularization, and is thus better suited to the regime with small n and large m . We apply an oracle version of M-GRAF which assumes knowledge of the true individual rank d_2 . Since M-GRAF does not assume a low-rank structure, it does not need a value for d_1 .

5.2 Gaussian model results

We consider instances of the Gaussian model with no self-loops, $d_1 = d_2 = 2$, and $\sigma = 1$, where we vary $n \in \{200, 300, 400, 500, 600\}$ with fixed $m = 8$, and vary $m \in \{4, 8, 12, 15, 20, 30\}$ with fixed $n = 400$. In each setting we generate 100 independent realizations from the model. The entries of the common and individual latent position matrices (V and $\{U_k\}_{k=1}^m$) are generated as independent standard normals, so while they are not strictly orthogonal, their expected correlation is 0. Under the Gaussian model, we have four methods to compare: the MultiNeSS estimator with and without the refitting step (denoted MultiNeSS and MultiNeSS+, respectively), the alternating rank truncation approach (SVD), and COSIE.

We evaluate the methods on how well they do on recovering the common structure, the individual structure, and the overall expectation of the adjacency matrix, using relative Frobenius norm errors

with $\|\cdot\|_{\tilde{F}}$ denoting the Frobenius norm which ignores diagonal entries:

$$\text{Err}_F := \frac{\|\hat{F} - F\|_{\tilde{F}}}{\|F\|_{\tilde{F}}}, \quad (23)$$

$$\text{Err}_G := \frac{1}{m} \sum_{k=1}^m \frac{\|\hat{G}_k - G_k\|_{\tilde{F}}}{\|G_k\|_{\tilde{F}}}, \quad (24)$$

$$\text{Err}_P := \frac{1}{m} \sum_{k=1}^m \frac{\|\hat{F} + \hat{G}_k - F - G_k\|_{\tilde{F}}}{\|F + G_k\|_{\tilde{F}}}. \quad (25)$$

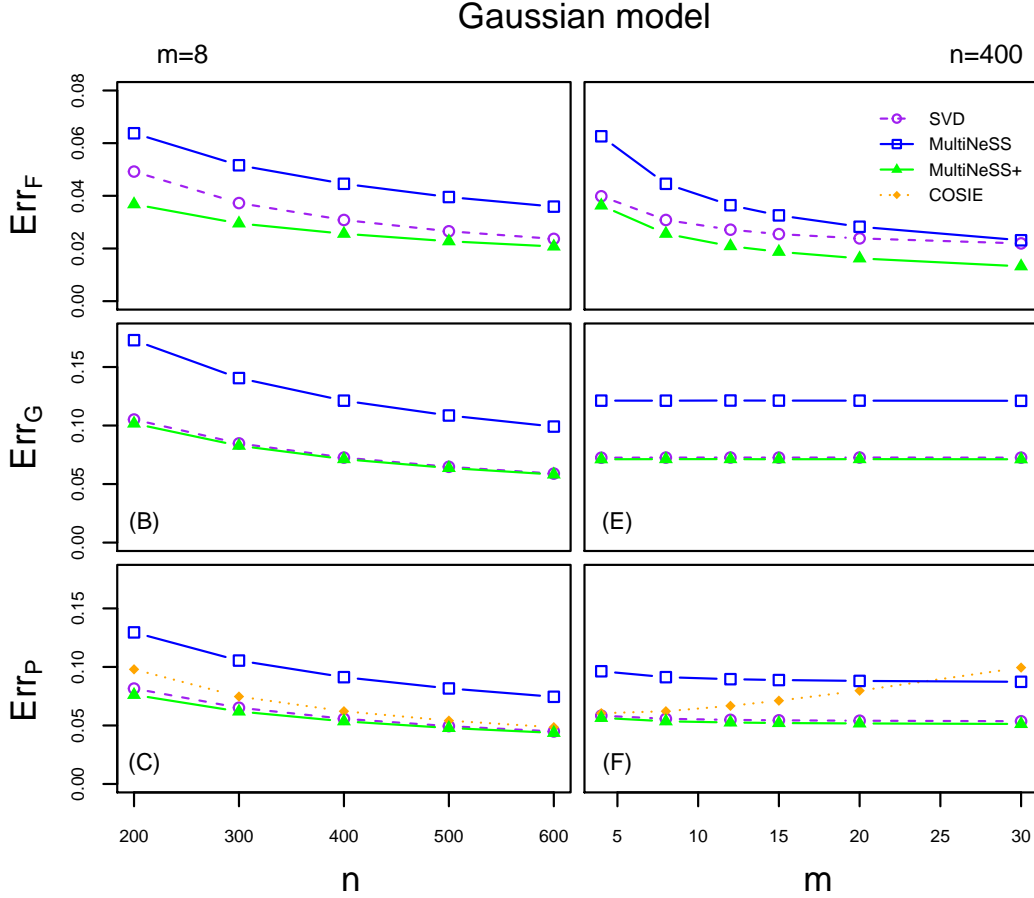


Figure 2: Frobenius norm errors for the common structure (top row), individual structure (middle row) and overall expected value (bottom row) under the Gaussian model.

The results are shown in Figure 2. Panels on the left (A, B, C) show the errors as a function of the number of nodes n , with the fixed number of layers $m = 8$. Panels on the right (D, E, F) show the errors as the number of layers m increases, with $n = 400$ fixed.

There are several general conclusions to draw here. MultiNeSS without the refitting step does not outperform SVD, but MultiNeSS+ is uniformly the best method in all cases, though SVD performs very similarly on estimating the individual layers G_k . One possible explanation for improvement over the SVD is that the convex optimization approach ignores the diagonal elements of the adjacency matrices, which do not reflect the true low-rank structure.

All methods perform better as the number of nodes n grows, as we would expect. The number of layers m growing has no effect on errors in estimating the individual components for MultiNeSS, since each one is estimated separately, but it helps us estimate F better by pooling shared information across more layers and therefore also improves the overall estimation of P . The rate of decrease in error in F seems to match well the rate of $m^{-1/2}$ predicted by the theory. COSIE, on the other hand, benefits from growing n but suffers when m grows, with the overall error in P going up with m . We conjecture that this happens because COSIE must first estimate a subspace of dimension $d_1 + m \cdot d_2$, which leads to high variability as m grows.

Comparing panel (C) to panels (A) and (B), and panel (F) to panels (D) and (E), we see that the estimation error for P_k is on average less than the estimation error for G_k , implying that the error in P_k does not decompose additively into error for G_k and error for F . Even when the expected correlation in the latent position matrices is zero, it is challenging to correctly distinguish common structure from individual structures.

5.3 Logistic model results

We also consider instances of the logistic model with no self-loops, and $d_1 = d_2 = 2$, where we vary $n \in \{200, 300, 400, 500, 600\}$ with fixed $m = 8$, and vary $m \in \{4, 8, 12, 15, 20, 30\}$ with fixed $n = 400$. In each setting we generate 100 independent realizations of the model. The entries of the common and individual latent position matrices (V and $\{U_k\}_{k=1}^m$) are generated as independent standard normals. We compare the MultiNeSS estimator with and without the refitting step (again denoted by MultiNeSS and MultiNeSS+) to the non-convex approach, COSIE, and M-GRAF. Note that COSIE does not use the correct model for this data since it assumes a random dot product graph model without a logistic link. We evaluate the recovery of the common and individual structures using the same relative Frobenius norm errors (23) and (24). To evaluate the overall recovery of the expected value for each layer, we use the relative Frobenius norm error after element-wise application of the inverse logistic link function

$$g(\mu) = \frac{e^\mu}{1 + e^\mu}.$$

That is, we redefine

$$\text{Err}_P := \frac{1}{m} \sum_{k=1}^m \frac{\|g(\hat{F} + \hat{G}_k) - g(F + G_k)\|_{\tilde{F}}}{\|g(F + G_k)\|_{\tilde{F}}}.$$

The results are shown in Figure 3. Panels on the left (A, B, C) show the errors as a function of the number of nodes n , with the fixed number of layers $m = 8$. Panels on the right (D, E, F) show the errors as the number of layers m increases, with $n = 400$ fixed.

Many of the general conclusions here are the same as for the Gaussian model. M-GRAF does not perform better as n increases, and performs much worse for small values of m , since it does not regularize the common matrix F in any way. In contrast to the Gaussian model, here the non-convex approach slightly outperforms MultiNeSS+. The difference between the non-convex and MultiNeSS+ errors is driven by large magnitude entries in F and G_k which have a substantial effect on the log-odds scale, but little effect on the expectation of the adjacency matrix. Hence, the difference between these two methods is attenuated in panels (C) and (F) after applying the inverse logistic link function.

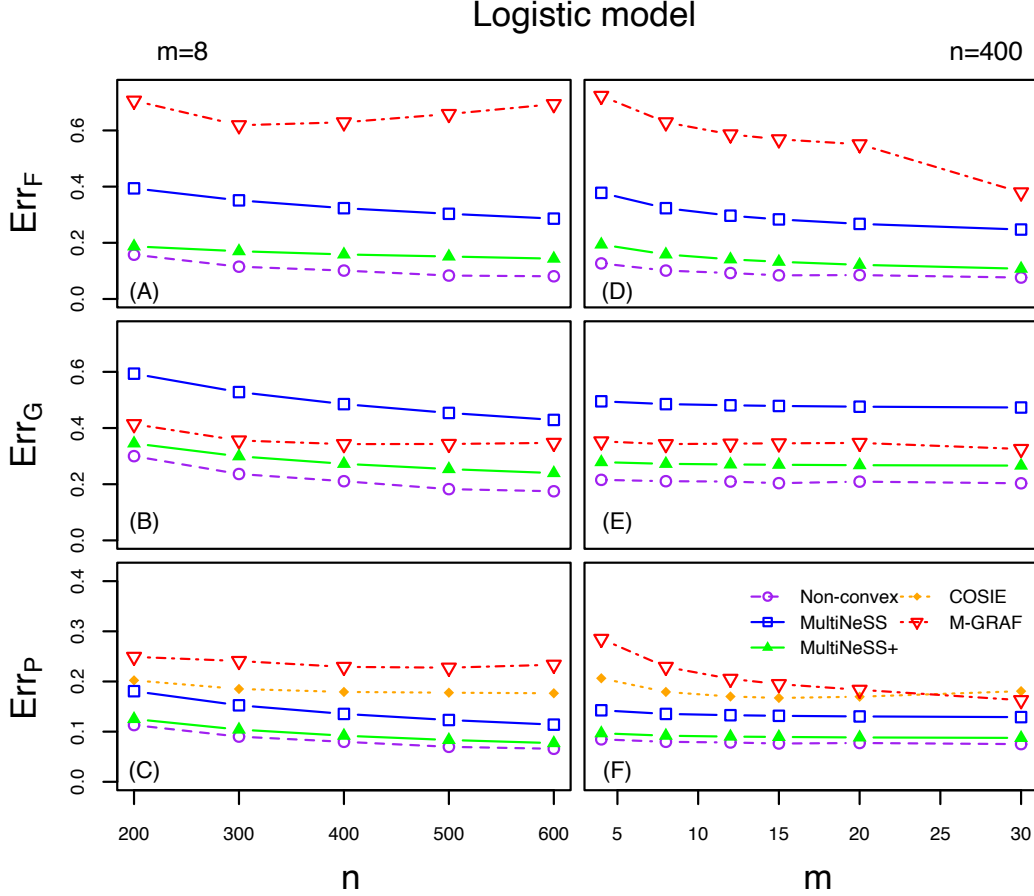


Figure 3: Frobenius norm errors for the common structure (top row), individual structure (middle row), and the overall expected value after the logistic transformation (bottom row), under the logistic model.

5.4 Dependent latent dimensions

In a final simulation study, we investigate the robustness of MultiNeSS to correlation among the latent dimensions, and its effect on recovery of the common structure matrix F in the large m regime. We consider instances of the Gaussian model as in Section 5.2 with $n = 200$, $d_1 = d_2 = 2$, $\sigma = 1$, and $m \in \{20, 50, 100, 150, 200, 300, 400, 600, 800, 1000\}$.

The entries of the common latent position matrix V are independent standard normals, while the individual latent position matrices U_k for $k = 1, \dots, m$ are generated as

$$U_k = \rho V \cdot O_k + \sqrt{1 - \rho^2} Z_k,$$

where $Z_k \in \mathbb{R}^{n \times 2}$ is a matrix with independent standard normal entries, and $O_k \in \mathbb{R}^{2 \times 2}$ are random orthonormal matrices generated uniformly from \mathcal{O}_2 . The parameter ρ controls the correlation amongst the individual latent dimensions, and between the common and individual latent dimensions. We evaluate the performance of MultiNeSS without the refitting step for $\rho \in \{0.2, 0.4, 0.6, 0.8\}$ using the non-normalized Frobenius norm errors for recovery of the common structure, and the overall expectation of the adjacency matrix. Tuning parameters are fixed as $\lambda = 2.309\sqrt{n}$ and $\alpha = \sqrt{m}$.

In the left panel of Figure 4, for $\rho = 0.2$, the error for F decreases monotonically in m , while for

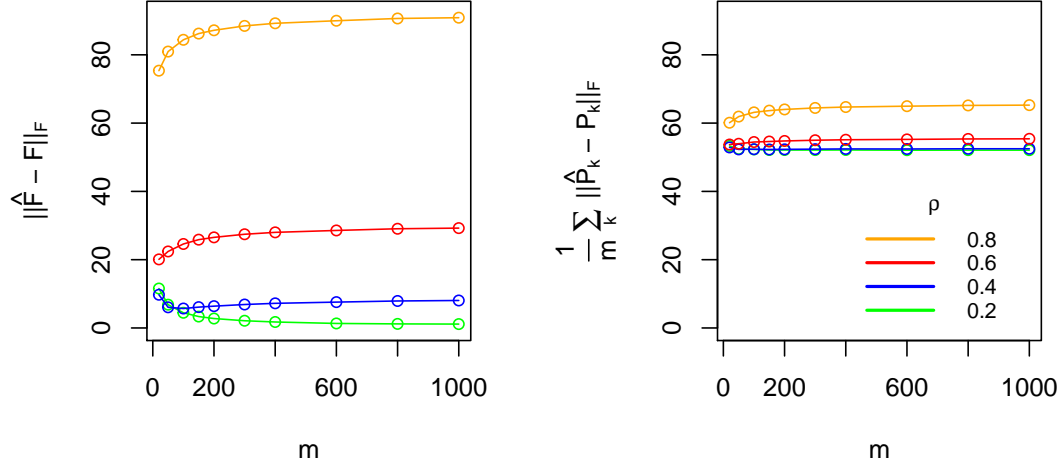


Figure 4: Frobenius norm errors for the common structure (left panel) and the overall expected value (right panel), under the Gaussian model.

$\rho \geq 0.6$ it increases in m . For $\rho = 0.4$, the error decreases in m for small m , but then reaches a minimum, and increases for larger values of m .

In the right panel of Figure 4, the error for the expected adjacency matrices $P_k = F + G_k$ is less sensitive to ρ , implying that the main source of error is incorrect allocation of structure between F and G_k , not recovery of the overall structure in each layer. The performance gap in the left panel between $\rho = 0.8$ and $\rho \leq 0.6$ occurs because the estimated individual matrices G_k do not have the correct rank. For large ρ , enough of the individual structure is included in the common latent position matrix that the remaining individual structure falls below the thresholding level. Note that even for $\rho = 0.2$, where the estimation error for F approaches zero as $m \rightarrow \infty$, the estimation error for P_k is lower bounded by the estimation error for G_k , which is at best constant in m .

6 An agricultural trade network analysis

As an illustration of insights one can gain from fitting a MultiNeSS model, we analyze a data set of food and agriculture trade relationships between countries, collected in 2010 [De Domenico et al., 2015]. Each node corresponds to a country, and each layer to a different agricultural product. The (undirected) edges are weighted by the quantity of the traded commodity. This data set has previously been analyzed by De Domenico et al. [2015], who looked at structural similarities between layers.

As a pre-processing step, we remove low density layers and nodes. The original dataset contains 214 countries and 364 products. We kept layers with overall edge density greater than 10%, and included nodes with average degree greater than 5 across these layers. The result is an undirected multiplex network with no self loops, with $n = 145$ nodes and $m = 13$ layers corresponding to agricultural products with high trade volume. Following common practice for this type of data, we work with log trade volumes as edge weights, which also makes the assumption of Gaussian edge weights with constant variance within each layer more realistic.

We fit a Gaussian model using the MultiNeSS algorithm with refitting. The tuning parameters are selected using the layer-specific adaptive tuning approach described in Section 3.4. The constant in (10) is set to $\delta = 1$ using edge cross-validation.

We show the results for the first four common latent dimensions (Figure 5) and the first two individual dimensions for two example layers, wine (Figure 6) and chocolate (Figure 7).

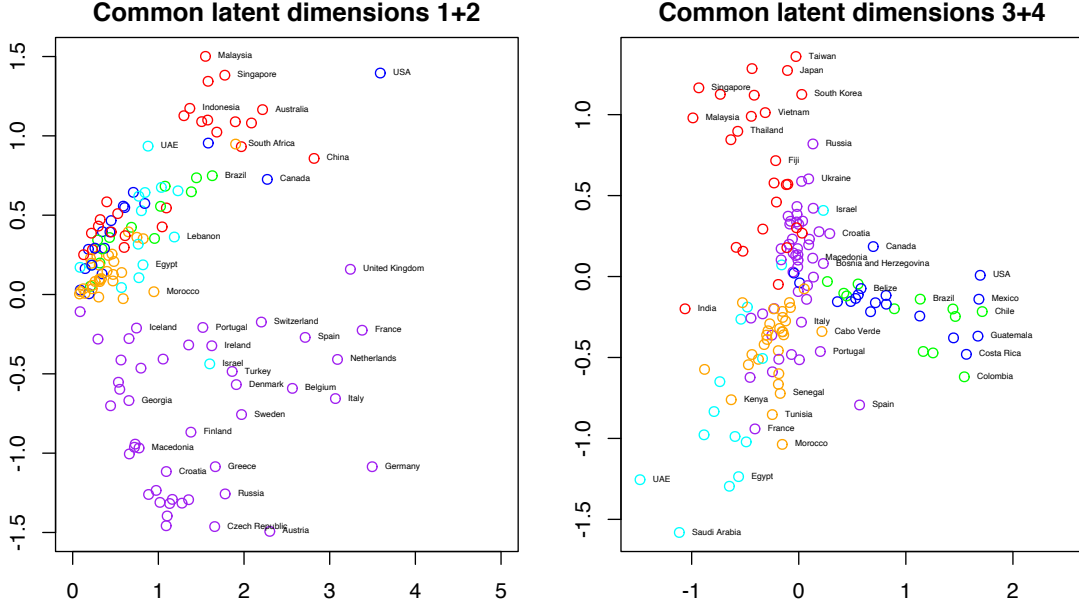


Figure 5: Scatter plots of first four MultiNeSS common latent dimensions of the food trade data. Left panel: dimensions 1 and 2, right panel: dimensions 3 and 4. Points are colored by geographical region. Orange: Africa, Red: Asia-Pacific, Purple: Europe, Cyan: Mid East, Blue: North America, Green: South America.

The estimated common matrix \hat{F} has rank 23. Figure 5 shows the scatter plots of the points projected onto the leading four latent dimensions (first and second on the left, third and fourth on the right). The first four eigenvalues account for approximately 50% of the trace of \hat{F} . The scatter plots suggest that the first latent dimension corresponds roughly to the total volume of trade, and the subsequent ones correspond to regional trade relationships. In particular, the second dimension primarily separates Europe from Asia, the third separates the Americas from the rest of the world, and the fourth separates the Middle East and Africa from Asia and the Pacific.

For the individual component of the wine trade layer (Figure 6), we estimate $\text{rank}(\hat{G}_{\text{wine}}) = 6$, and plot the scatter plot on the first two latent dimensions, which account for about 61% of the trace of \hat{G}_{wine} . The first latent dimension corresponds roughly to the total volume of wine trade, with countries like France, Spain, Chile, and New Zealand with very high scores, and countries in the Middle East like Saudi Arabia with very low scores. The second latent dimension captures regional patterns between high volume wine importers (Russia, Canada, Netherlands, China, Denmark) and high volume exporters which are atypical relative to usual global agricultural trade.

For comparison, we also plot the countries projected onto the first two latent dimensions constructed by adjacency spectral embedding (ASE) applied to just the wine trade network. It appears that accounting for the overall shared trade patterns first helps identify patterns specific to wine and separate them from general regional patterns better (for example, the big wine producing countries like France still score high on the first ASE latent dimension, but so do other European countries like the UK which do not produce much wine). The second latent dimension for ASE appears to

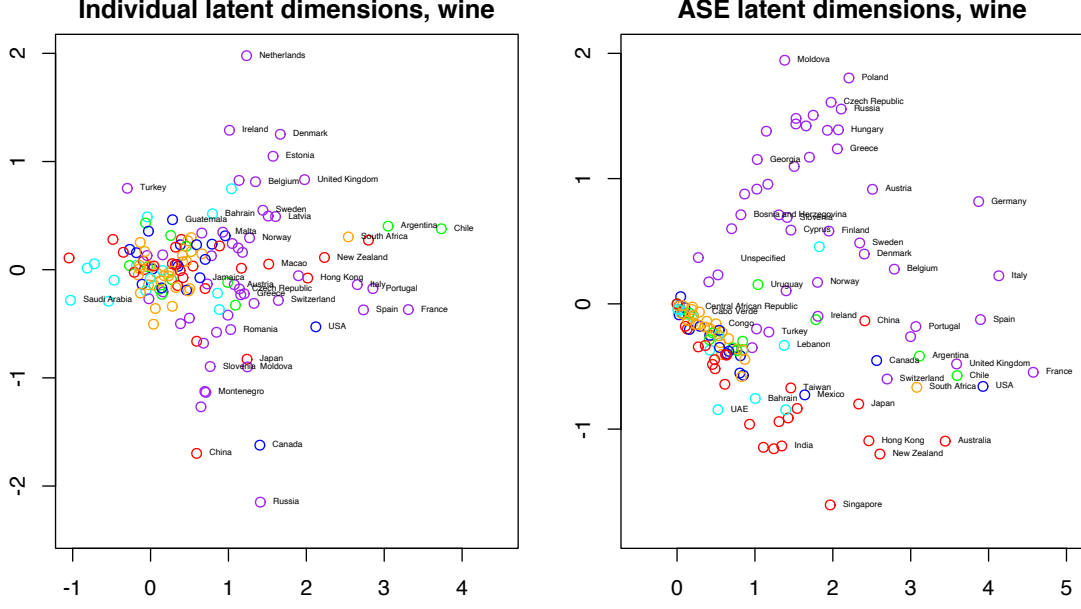


Figure 6: Scatter plots of first two individual latent dimensions, wine layer. Left panel: dimensions 1 and 2 by MultiNeSS, right panel: dimensions 1 and 2 by adjacency spectral embedding. Points are colored by geographical region. Orange: Africa, Red: Asia-Pacific, Purple: Europe, Cyan: Middle East, Blue: North America, Green: South America.

primarily separate Europe from the Asia-Pacific region, which is not necessarily wine-specific.

For the chocolate trading network, we estimate the individual component rank as $\text{rank}(\hat{G}_{\text{chocolate}}) = 4$. Projections on to the first two individual latent dimensions, which account for about 73% of the trace of $\hat{G}_{\text{chocolate}}$, are shown in Figure 7. Overall, the pattern is similar to what we saw for wine in Figure 6, with the first latent dimension identifying chocolate producing nations like Switzerland and Belgium with the highest scores, and countries like Vietnam, which has a very low per capita chocolate consumption, with the lowest score. The second dimension appears to identify a regional split, between Europe and South America. As in the wine layer, these chocolate-specific patterns are far less apparent in the scatter plot from the adjacency spectral embedding which does not account for the shared structure.

As a quantitative demonstration of our shared structure modeling approach, we also apply it to an edge imputation task. For $k = 1, \dots, 13$ layers, some proportion p of non-zero edges in layer k are held out, while the other layers are left fully observed. We compare the MultiNeSS estimator to standard low-rank matrix imputation by singular value thresholding (see for instance Li et al. [2020]), denoted below by SVD, which does not incorporate information from the other layers.

From Figure 8, we see that MultiNeSS is insensitive to the proportion of edges missing compared to singular value thresholding. In all layers MultiNeSS strictly dominates singular value thresholding, demonstrating the benefit of pooling information across layers, and validating the modeling assumption that there is common structure across all the layers of this multiplex network.

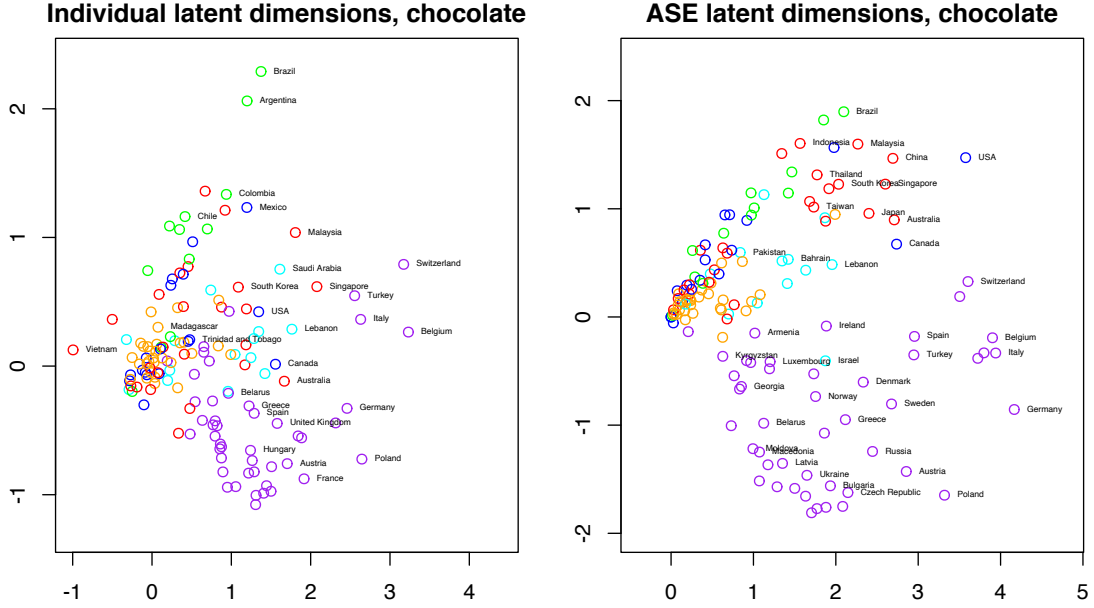


Figure 7: Scatter plots of first two individual latent dimensions, chocolate layer. Left panel: dimensions 1 and 2 by MultiNeSS, right panel: dimensions 1 and 2 by adjacency spectral embedding. Points are colored by geographical region. Orange: Africa, Red: Asia-Pacific, Purple: Europe, Cyan: Mid East, Blue: North America, Green: South America.

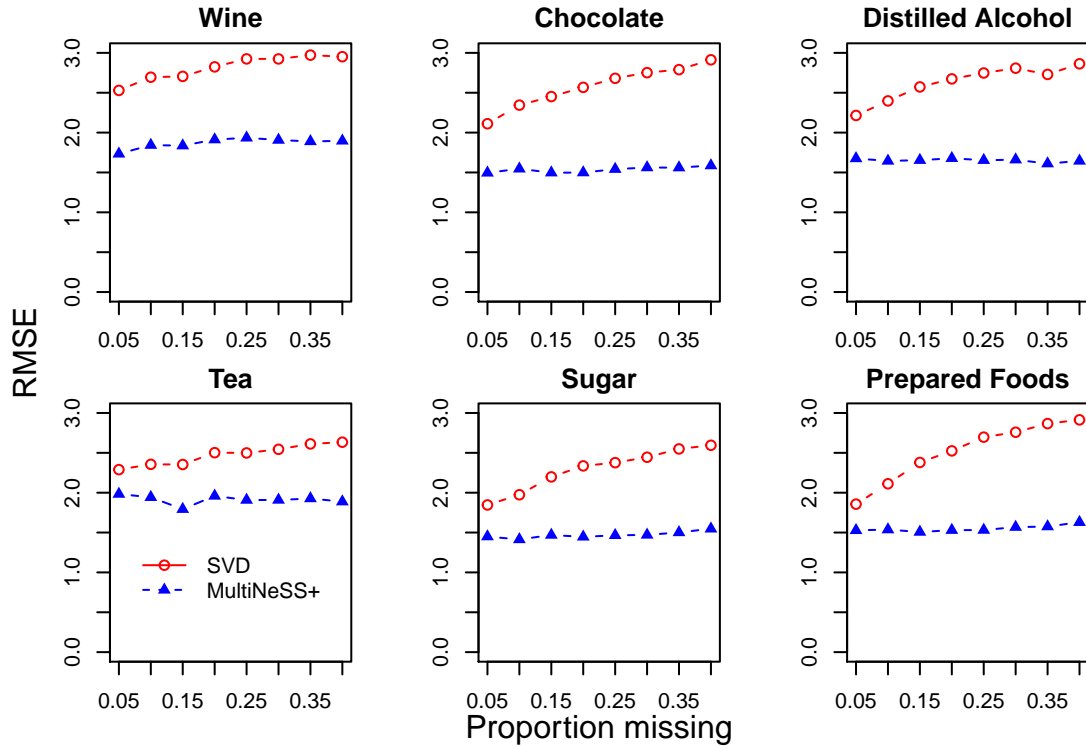


Figure 8: Comparison of edge imputation performance (RMSE) for a selection of six layers.

7 Discussion

The central contribution of this work is MultiNeSS, a latent space model for multiplex networks with shared structure which allows for learning both common and individual structure in the layers. The model can be fitted with a convex optimization algorithm, and an additional fast de-biasing step can improve its fit. The algorithm is data-driven and can adapt to different levels of noise at different edges. We allow for general edge weight distributions and general similarity functions between latent positions as the center parameter of the distribution. For the case of similarity measured by inner product, we prove the identifiability of the model under a mild linear independence condition that does not require orthogonality of the common and individual latent dimension, and for the Gaussian model of edge weights, we establish consistency of our estimators. We expect this can be extended to other well-behaved edge weight distributions. We demonstrate the method’s effectiveness over existing methods on simulated multiplex networks and on a food trading network, where it produces interpretable insights distinct from what one can get from separate analysis. MultiNeSS can easily handle missing entries and edge imputation, with quantitative improvement compared to standard matrix completion techniques which do not pool information across layers.

There are several directions in which we plan to take this work forward. The models we developed so far allow for only two kinds of latent dimensions: those which are individual to one layer, and those which are common to all layers. Extending this to more structured models, where latent dimensions can be shared by some but not all layers, would allow for a larger range of applications. For example, we could impose a group structure on the layers, allowing for group effects and enabling an analogue to ANOVA on networks. An example application where this would be very useful is neuroimaging, where brain connectivity networks of a treatment group and a control group of patients could be analyzed jointly and the treatment effect estimated more accurately. These groups could also be learned from data, in a natural extension of this setup to clustering.

Another possible extension is to dynamic networks, where each layer represents a network snapshot at a discrete time point. In this setting, unlike in ours, the ordering of the layers matters. Latent dimensions could be modeled as constant over time or constant over a contiguous time window, with obvious applications to prediction and change-point analysis. Finally, a highly interpretable latent structure could be obtained if we imposed a tree structure on the latent dimensions, with shared latent dimensions between nodes determined by their last common ancestor on the tree.

While this work focuses on latent space models with the inner product similarity function, the framework is general and can work with other similarity functions. As an example, since the inner product restricts the fixed effect matrices F and G_k to be positive semi-definite, it could be replaced by a signed inner product similarity function [Rubin-Delanchy et al., 2017], of the form

$$\kappa_{p,d}(x, y) = x_1y_1 + \cdots + x_py_p - x_{p+1}y_{p+1} - \cdots - x_dy_d.$$

This similarity function would allow the matrices F and G_k to have negative eigenvalues, making it possible to model disassortative latent dimensions, and again increase the range of potentially impactful applications.

References

- J. Arroyo, A. Athreya, J. Cape, G. Chen, C. E. Priebe, and J. T. Vogelstein. Inference for multiple heterogeneous networks with a common invariant subspace. *arXiv preprint arXiv:1906.10026*, 2019.

- A. Athreya, D. E. Fishkind, M. Tang, C. E. Priebe, Y. Park, J. T. Vogelstein, K. Levin, V. Lyzinski, and Y. Qin. Statistical inference on random dot product graphs: a survey. *The Journal of Machine Learning Research*, 18(1):8393–8484, 2017.
- A. S. Bandeira and R. Van Handel. Sharp nonasymptotic bounds on the norm of random matrices with independent entries. *The Annals of Probability*, 44(4):2479–2506, 2016.
- R. Bhatia. *Matrix Analysis*, volume 169. Springer Science & Business Media, 2013.
- P. Bickel, D. Choi, X. Chang, and H. Zhang. Asymptotic normality of maximum likelihood and its variational approximation for stochastic blockmodels. *The Annals of Statistics*, 41(4):1922–1943, 2013.
- T. T. Cai and A. Zhang. Rate-optimal perturbation bounds for singular subspaces with applications to high-dimensional statistics. *The Annals of Statistics*, 46(1):60–89, 2018.
- J. Cape, M. Tang, and C. E. Priebe. The two-to-infinity norm and singular subspace geometry with applications to high-dimensional statistics. *The Annals of Statistics*, 47(5):2405–2439, 2019.
- S. Chatterjee. Matrix estimation by universal singular value thresholding. *The Annals of Statistics*, 43(1):177–214, 2015.
- M. De Domenico, V. Nicosia, A. Arenas, and V. Latora. Structural reducibility of multilayer networks. *Nature Communications*, 6(1):1–9, 2015.
- S. D’Angelo, T. B. Murphy, M. Alfò, et al. Latent space modelling of multidimensional networks with application to the exchange of votes in Eurovision song contest. *The Annals of Applied Statistics*, 13(2):900–930, 2019.
- W. Fithian and R. Mazumder. Flexible low-rank statistical modeling with missing data and side information. *Statistical Science*, 33(2):238–260, 2018.
- M. Gavish and D. L. Donoho. The optimal hard threshold for singular values is $4/\sqrt{3}$. *IEEE Transactions on Information Theory*, 60(8):5040–5053, 2014.
- I. Gollini and T. B. Murphy. Joint modeling of multiple network views. *Journal of Computational and Graphical Statistics*, 25(1):246–265, 2016.
- M. S. Handcock, A. E. Raftery, and J. M. Tantrum. Model-based clustering for social networks. *Journal of the Royal Statistical Society: Series A (Statistics in Society)*, 170(2):301–354, 2007.
- P. D. Hoff, A. E. Raftery, and M. S. Handcock. Latent space approaches to social network analysis. *Journal of the American Statistical Association*, 97(460):1090–1098, 2002.
- P. W. Holland, K. B. Laskey, and S. Leinhardt. Stochastic blockmodels: First steps. *Social networks*, 5(2):109–137, 1983.
- B. Kim, K. H. Lee, L. Xue, and X. Niu. A review of dynamic network models with latent variables. *Statistics Surveys*, 12:105, 2018.
- M. Kivelä, A. Arenas, M. Barthélemy, J. P. Gleeson, Y. Moreno, and M. A. Porter. Multilayer networks. *Journal of Complex Networks*, 2(3):203–271, 2014.
- V. Koltchinskii, K. Lounici, and A. B. Tsybakov. Nuclear-norm penalization and optimal rates for noisy low-rank matrix completion. *The Annals of Statistics*, 39(5):2302–2329, 2011.

- J. Lei and A. Rinaldo. Consistency of spectral clustering in stochastic block models. *The Annals of Statistics*, 43(1):215–237, 2015.
- K. Levin, A. Athreya, M. Tang, V. Lyzinski, and C. E. Priebe. A central limit theorem for an omnibus embedding of multiple random dot product graphs. In *2017 IEEE International Conference on Data Mining Workshops (ICDMW)*, pages 964–967. IEEE, 2017.
- T. Li, E. Levina, and J. Zhu. Network cross-validation by edge sampling. *Biometrika*, 107(2): 257–276, 2020.
- E. F. Lock, J. Y. Park, and K. A. Hoadley. Bidimensional linked matrix factorization for pan-omics pan-cancer analysis. *arXiv preprint arXiv:2002.02601*, 2020.
- Z. Ma, Z. Ma, and H. Yuan. Universal latent space model fitting for large networks with edge covariates. *Journal of Machine Learning Research*, 21(4):1–67, 2020.
- C. Matias and S. Robin. Modeling heterogeneity in random graphs through latent space models: a selective review. *ESAIM: Proceedings and Surveys*, 47:55–74, 2014.
- R. Mazumder, T. Hastie, and R. Tibshirani. Spectral regularization algorithms for learning large incomplete matrices. *Journal of Machine Learning Research*, 11:2287–2322, 2010.
- A. M. Nielsen and D. Witten. The multiple random dot product graph model. *arXiv preprint arXiv:1811.12172*, 2018.
- P. Rubin-Delanchy, C. E. Priebe, M. Tang, and J. Cape. A statistical interpretation of spectral embedding: the generalised random dot product graph. *arXiv preprint arXiv:1709.05506*, 2017.
- M. Salter-Townshend and T. H. McCormick. Latent space models for multiview network data. *The Annals of Applied Statistics*, 11(3):1217, 2017.
- M. Tang, D. L. Sussman, and C. E. Priebe. Universally consistent vertex classification for latent positions graphs. *The Annals of Statistics*, 41(3):1406–1430, 2013.
- L. Wang, Z. Zhang, and D. Dunson. Common and individual structure of brain networks. *The Annals of Applied Statistics*, 13(1):85–112, 2019a.
- S. Wang, J. Arroyo, J. T. Vogelstein, and C. E. Priebe. Joint embedding of graphs. *IEEE Transactions on Pattern Analysis and Machine Intelligence*, 2019b.
- Y.-J. Wu, E. Levina, and J. Zhu. Generalized linear models with low rank effects for network data. *arXiv preprint arXiv:1705.06772*, 2017.
- S. J. Young and E. R. Scheinerman. Random dot product graph models for social networks. In *International Workshop on Algorithms and Models for the Web-Graph*, pages 138–149. Springer, 2007.
- X. Zhang, S. Xue, and J. Zhu. A flexible latent space model for multilayer networks. In *International Conference on Machine Learning*, pages 11288–11297. PMLR, 2020.

A Details of proximal gradient descent

Recall that we split the optimization variables into $m + 1$ blocks of $\binom{n}{2}$ variables: one block containing the entries of F ; and one block each for the entries of G_k , $k = 1, \dots, m$. For each block $j = 0, \dots, m + 1$, define $h_{j,1}$, the smooth part of (4) written as a function of block j , and $h_{j,2}$, the part of the penalty which depends on block j :

$$\begin{aligned} h_{0,1}(F) + h_{0,2}(F) &= -\frac{1}{2} \sum_{m=1}^M \sum_{i \neq j} \log Q(A_{k,ij}; F_{ij} + G_{k,ij}) + \lambda \alpha \|F\|_* , \\ h_{k,1}(G) + h_{k,2}(G) &= -\frac{1}{2} \sum_{i \neq j} \log Q(A_{k,ij}; F_{ij} + G_{k,ij}) + \lambda \|G\|_* \text{ for } k = 1, \dots, m. \end{aligned}$$

Then for $k = 0, \dots, m$, $h_{k,1}$ is convex and differentiable, and $h_{k,2}$ is convex and, although non-differentiable, has a well-defined proximal mapping for step size η [Fithian and Mazumder, 2018]. In particular, the nuclear norm scaled by $\lambda \geq 0$ has the proximal mapping

$$\operatorname{argmin}_{F'} \frac{1}{2\eta} \|F - F'\|_F^2 + \lambda \|F'\|_* = S_{\eta\lambda}(F) ,$$

where $S_T(\cdot)$ is the soft singular value thresholding operator with threshold $T \geq 0$. A similar proximal mapping follows for $k = 1, \dots, m$. Differentiating $h_{k,1}$ for $k = 0, \dots, m$ gives

$$\begin{aligned} \frac{\partial h_{0,1}}{\partial F_{ij}} &= -\sum_{k=1}^m (\log Q)'(A_{k,ij}; F_{ij} + G_{k,ij}) \\ \frac{\partial h_{k,1}}{\partial G_{k,ij}} &= -(\log Q)'(A_{k,ij}; F_{ij} + G_{k,ij}) \end{aligned}$$

if $i \neq j$, and

$$\frac{\partial h_{0,1}}{\partial F_{ii}} = \frac{\partial h_{k,1}}{\partial G_{k,ii}} = 0 \quad (26)$$

otherwise. We select the relative step sizes based on the Lipschitz constants of each block objective. If $\log Q$ is Lipschitz in μ with constant L , then $h_{0,1}$ has Lipschitz constant $L_0 = mL$, while $h_{k,1}$ for $k \geq 1$ has Lipschitz constant $L_k \equiv L$. Thus proximal gradient descent with scaled step size $L\eta/L_k$ gives the following update steps: for iteration number $t \geq 1$,

$$\hat{F}^{(t)} = S_{\eta\lambda\alpha/m} \left(\hat{F}^{(t-1)} - \frac{\eta}{m} \frac{\partial h_{0,1}(\hat{F}^{(t-1)})}{\partial F} \right) , \quad (27)$$

$$\hat{G}_k^{(t)} = S_{\eta\lambda} \left(\hat{G}_k^{(t-1)} - \eta \frac{\partial h_{k,1}(\hat{G}_k^{(t-1)})}{\partial G_k} \right) \text{ for } k = 1, \dots, m. \quad (28)$$

B Proofs

B.1 Proof of Proposition 1

Proof of Proposition 1. For $1 \leq k \leq m$, each matrix $VV^\top + U_k U_k^\top$ is identifiable and $\begin{bmatrix} V & U_k \end{bmatrix}$ has linearly independent columns, thus by Lemma A.1 of Tang et al. [2013],

$$\begin{bmatrix} V & U_k \end{bmatrix} O_k = \begin{bmatrix} V' & U'_k \end{bmatrix} \quad (29)$$

for some orthogonal matrix $O_k \in \mathbb{R}^{d \times d}$. It suffices to show that O_k has the block structure

$$O_k = \begin{bmatrix} O_{11,k} & O_{12,k} \\ O_{21,k} & O_{22,k} \end{bmatrix} = \begin{bmatrix} O_{11} & 0 \\ 0 & O_{22,k} \end{bmatrix}. \quad (30)$$

Let $o_{k,\ell} \in \mathbb{R}^d$ denote the ℓ th column of O_k . We will apply the following argument for each of the pairs of layers $\{1, 2\}, \{2, 3\}, \dots, \{m-1, m\}$. Write

$$o_{k,\ell} = \begin{bmatrix} o_{k,\ell}^{(1)} \\ o_{k,\ell}^{(2)} \end{bmatrix} \in \mathbb{R}^{d_1} \times \mathbb{R}^{d_2}.$$

By (29),

$$0 = V(o_{1,\ell}^{(1)} - o_{2,\ell}^{(1)}) + U_1 o_{1,\ell}^{(2)} - U_2 o_{2,\ell}^{(2)},$$

and by (2), $o_{1,\ell}^{(1)} - o_{2,\ell}^{(1)} = 0$ and $o_{1,\ell}^{(2)} = o_{2,\ell}^{(2)} = 0$. Since this holds for all $\ell \in \{1, \dots, d_1\}$, we can conclude

$$\begin{aligned} O_{11,1} &= O_{11,2}, \\ O_{21,1} &= O_{21,2} = 0, \end{aligned}$$

and by orthonormality,

$$O_{12,1} = O_{12,2} = 0.$$

Applying this argument for each of the pairs of layers $\{1, 2\}, \{2, 3\}, \dots, \{m-1, m\}$ gives that $O_{11,k}$ is constant in k , and the off-diagonal blocks are zero for each k , which completes the proof by (30). \square

B.2 Proof of Theorem 1

Proof of Theorem 1. We first outline the entire proof, which will use several technical lemmas to come later. Let

$$\begin{aligned} \mathcal{E}_0 &= \left\{ \left\| \sum_k E_k \right\|_2 \leq 3\sigma\sqrt{mn} \right\}, \\ \mathcal{E}_k &= \left\{ \|E_k\|_2 \leq 3\sigma\sqrt{n} \right\} \text{ for } k = 1, \dots, m. \end{aligned}$$

and define the event

$$\mathcal{E} = \cap_{k=0}^m \mathcal{E}_k. \quad (31)$$

We will first show in Lemma 2 that $\mathbb{P}(\mathcal{E}) > 1 - (m+1)ne^{-C_0 n}$ for some universal constant C_0 . For the remainder of the proof we assume that \mathcal{E} holds.

Next, Lemma 6 establishes the error rate (17) for the initializer when \mathcal{E} holds. Then Lemmas 7 and 15 show that after one iteration of proximal gradient descent, $\hat{F}^{(1)}$ and $\hat{G}_k^{(1)}$ satisfy the error bounds (18), and are positive semi-definite when \mathcal{E} holds. Moreover, by Assumption 1,

$$\|\hat{F}^{(1)} - F\|_F = o(n^{1/2}),$$

so treating $\hat{F}^{(1)}$ as the new initializer, the arguments in Lemmas 7 and 15 can be repeated to establish by induction (18) for \hat{F} and \hat{G}_k , the limits of the proximal gradient descent algorithm. \square

Throughout this subsection, we let C denote an arbitrary positive constant which is free of the parameters (n, m, d_1, d_2, σ) . Since the proofs of Lemmas 7-15 only utilize the estimators after one proximal gradient step, to simplify notation we omit the superscript ‘(1)’ for the estimators $\hat{F}^{(1)}$ and $\{\hat{G}_k^{(1)}\}_{k=1}^m$. First, we state a technical lemma from [Bandeira and Van Handel \[2016\]](#) we will use below.

Lemma 1 ([Bandeira and Van Handel \[2016\]](#), Corollary 3.9). Let $M \in \mathbb{R}^{n \times n}$ be a symmetric matrix with entries

$$M_{ij} = b_{ij}g_{ij},$$

where $\{g_{ij} : i \leq j\}$ are iid standard normal random variables, and $\{b_{ij} : i \leq j\}$ are fixed scalars. Define

$$\begin{aligned}\sigma_* &= \max_i \sqrt{\sum_j b_{ij}^2}, \\ \sigma_{**} &= \max_{ij} |b_{ij}|.\end{aligned}$$

Then for every $\epsilon \in (0, 1/2]$, there exists a constant c_ϵ such that for every $t \geq 0$,

$$\mathbb{P}(\|M\|_2 \geq (1 + \epsilon)2\sigma_* + t) \leq n \exp \left\{ -\frac{t^2}{c_\epsilon \sigma_{**}^2} \right\}. \quad (32)$$

Using Lemma 1, we next establish Lemma 2, which shows the event \mathcal{E} holds with high probability.

Lemma 2. Define the event \mathcal{E} as in (31). Then

$$\mathbb{P}(\mathcal{E}) \geq 1 - (m + 1)ne^{-C_0 n},$$

for some universal constant $C_0 > 0$.

Proof of Lemma 2. We first show the desired event for each individual error matrix. Fix some $k \in \{1, \dots, m\}$. Using the notation of Proposition 1 for the matrix E_k ,

$$\sigma_* = \sigma\sqrt{n-1}, \quad \sigma_{**} = \sigma.$$

Specify $\epsilon = 1/4$ and $t = \sigma\sqrt{n}/4$. Then by Proposition 1,

$$\mathbb{P}\left(\|E_k\|_2 \leq \frac{11}{4}\sigma\sqrt{n}\right) \geq 1 - n \exp\{-C_0 n\}$$

for some constant $C_0 > 0$. In particular, C_0 is the universal constant $c_{1/4}$ corresponding to the choice of $\epsilon = 1/4$ in Proposition 1. For the matrix $\sum_k E_k$, the entries are independent with variance

m , so

$$\sigma_* = \sigma\sqrt{m(n-1)}, \quad \sigma_{**} = \sigma\sqrt{m},$$

and the same proof gives

$$\mathbb{P}\left(\left\|\sum_k E_k\right\|_2 \leq 3\sigma\sqrt{mn}\right) \geq 1 - n \exp\{-C_0 n\}.$$

The proof is complete by a union bound. \square

The next two technical lemmas will be used repeatedly to control the operator norm of a sum of square matrices. Lemma 3 provides a tighter bound when the matrices are symmetric and positive semi-definite, while Lemma 4 applies in the general non-symmetric case.

Lemma 3. Suppose $\{M_k\}_{k=1}^m \subset \mathbb{R}^{n \times n}$ are symmetric and positive semi-definite matrices with eigendecompositions

$$M_k = U_k \Lambda_k U_k^\top,$$

which satisfy

$$\max_k \|\Lambda_k\|_2 \leq \tau, \tag{33}$$

$$\max_{k_1 \neq k_2} \|U_{k_1}^\top U_{k_2}\|_2 \leq \gamma. \tag{34}$$

Then

$$\left\|\sum_k M_k\right\|_2 \leq \tau(1 - \gamma) + m\tau\gamma \leq \tau(1 + m\gamma). \tag{35}$$

Proof of Lemma 3.

$$\sum_k M_k = \begin{bmatrix} U_1 \Lambda_1^{1/2} & \cdots & U_m \Lambda_m^{1/2} \end{bmatrix} \begin{bmatrix} U_1 \Lambda_1^{1/2} & \cdots & U_m \Lambda_m^{1/2} \end{bmatrix}^\top,$$

Then $\sum_k M_k$ has the same singular values as the $mn \times mn$ matrix

$$\mathcal{M} := \begin{bmatrix} \Lambda_1^{1/2} U_1^\top U_1 \Lambda_1^{1/2} & \Lambda_1^{1/2} U_1^\top U_2 \Lambda_2^{1/2} & & \\ \Lambda_2^{1/2} U_2^\top U_1 \Lambda_1^{1/2} & \ddots & & \\ & & \ddots & \\ & & & \Lambda_m^{1/2} U_m^\top U_m \Lambda_m^{1/2} \end{bmatrix}.$$

To bound the largest singular value of this matrix, we decompose it into m summands and use the triangle inequality.

$$\left\|\sum_k M_k\right\|_2 = \|\mathcal{M}\|_2 \leq \sum_{j=0}^{m-1} \left\| \text{diag} \left(\left\{ \Lambda_k^{1/2} U_k^\top U_{k+j} \Lambda_{k+j}^{1/2} \right\}_{k=1}^m \right) \right\|_2, \tag{36}$$

where the indices are interpreted modulo m and diag constructs a block diagonal matrix.

In the sum on the right-hand side of (36), $j = 0$ corresponds to the main diagonal, and by the submultiplicative property, the largest singular value is bounded by τ . For the $m - 1$ other terms, every non-zero block contains $U_i^\top U_{i'}$ for some $i \neq i'$, so again using submultiplicativity, the largest

singular value is bounded by $\tau\gamma$. Thus we get the desired bound,

$$\left\| \sum_k M_k \right\|_2 \leq \tau(1 - \gamma) + m\tau\gamma.$$

□

Lemma 4. Suppose $\{M_k\}_{k=1}^m \subset \mathbb{R}^{n \times n}$ are matrices which satisfy $\max_k \|M_k\|_2 \leq \tau$, and either

$$\max_{k_1 \neq k_2} \|M_{k_1}^\top M_{k_2}\|_2 \leq \tau^2\gamma, \quad (37)$$

or

$$\max_{k_1 \neq k_2} \|M_{k_1} M_{k_2}^\top\|_2 \leq \tau^2\gamma. \quad (38)$$

Then

$$\left\| \sum_k M_k \right\|_2 \leq m^{1/2} \tau (1 + m\gamma)^{1/2}. \quad (39)$$

Proof of Lemma 4. Suppose (37) holds. Then

$$\begin{aligned} \left\| \sum_k M_k \right\|_2^2 &= \gamma_1 \left(\left(\sum_k M_k \right)^\top \left(\sum_k M_k \right) \right) = \left\| \sum_{i=1}^m \sum_{j=1}^m M_i^\top M_j \right\|_2 \\ &\leq \sum_{i=1}^m \sum_{j=1}^m \|M_i^\top M_j\|_2 = \sum_{i=1}^m \|M_i^\top M_i\|_2 + \sum_{i=1}^m \sum_{j \neq i}^m \|M_i^\top M_j\|_2 \\ &\leq m\tau^2 (1 + m\gamma). \end{aligned}$$

If instead (38) holds, the same argument can be made beginning with

$$\left\| \sum_k M_k \right\|_2^2 = \gamma_1 \left(\left(\sum_k M_k \right) \left(\sum_k M_k \right)^\top \right).$$

□

In Lemmas 5 and 6, we establish the bound (17) for the error of initializer, which will rely on an application of Cai and Zhang [2018], Theorem 1.

Lemma 5. Suppose the assumptions of Theorem 1 hold, and suppose \mathcal{E} holds. Let \hat{V}_0 denote the matrix containing the first d_1 eigenvectors of $\frac{1}{m} \sum_k A_k$. Then for sufficiently large n ,

$$\|\hat{V}_0 \hat{V}_0^\top - \bar{V} \bar{V}^\top\|_2 = \|\sin \Theta(\bar{V}, \hat{V}_0)\|_2 = o(d_1^{-1/2} n^{1/2-\tau}) \quad (40)$$

Proof of Lemma 5. We need to lower bound the smallest non-zero singular value of

$$\bar{V}^\top \left(\frac{1}{m} \sum_k A_k \right) \bar{V},$$

which is at least

$$b_1 n^\tau - \left\| \frac{1}{m} \sum_k G_k \right\|_2 - \left\| \frac{1}{m} \sum_k E_k \right\|_2. \quad (41)$$

Suppose \bar{V}_\perp is an orthonormal basis for the complement of $\text{col}(F)$. We also need to upper bound the largest singular value of

$$\bar{V}_\perp^\top \left(\frac{1}{m} \sum_k A_k \right) \bar{V}_\perp,$$

which is at most

$$\left\| \frac{1}{m} \sum_k G_k \right\|_2 + \left\| \frac{1}{m} \sum_k E_k \right\|_2. \quad (42)$$

Since each G_k is symmetric and positive semi-definite, by Lemma 3,

$$\left\| \sum_k G_k \right\|_2 \leq Cn^\tau \left(1 + \sigma mn^{1/2-\tau} \right)$$

for a constant $C > 0$. Thus the first term in (42) is $o(n^\tau)$. Similarly, the second term is $o(n^\tau)$.

Finally, we need to control the operator norm $\left\| \sum_k \bar{V} \bar{V}^\top G_k \right\|_2$. For any k ,

$$\left\| \bar{V} \bar{V}^\top \bar{U}_k \Gamma_k \bar{U}_k^\top \right\|_2 \leq \left\| \bar{V}^\top \bar{U}_k \right\|_2 \left\| \Gamma_k \right\|_2 = o(d_1^{-1/2} m^{1/2} n^{1/2}),$$

and for and $k_1 \neq k_2$,

$$\left\| \bar{V} \bar{V}^\top G_{k_1} G_{k_2}^\top \bar{V} \bar{V}^\top \right\|_2 \leq \left\| \bar{V}^\top \bar{U}_{k_1} \right\|_2 \left\| \Gamma_{k_1} \right\|_2 \left\| \bar{U}_{k_1}^\top \bar{U}_{k_2} \right\|_2 \left\| \Gamma_{k_2} \right\|_2 \left\| \bar{U}_{k_2}^\top \bar{V} \right\|_2 = o\left(d_1^{-1} mn \cdot n^{1/2-\tau}\right).$$

Then by Lemma 4, since $mn^{1/2-\tau} \rightarrow 0$, we have

$$\left\| \sum_k \bar{V} \bar{V}^\top G_k \right\|_2 = o(d_1^{-1/2} mn^{1/2}),$$

and the result is a direct application of Cai and Zhang [2018], Theorem 1 (for sufficiently large n). \square

Lemma 6. Denote $\Delta_{F_0} = \hat{F}^{(0)} - F$. Suppose the assumptions of Theorem 1 hold, and suppose \mathcal{E} holds. Then for sufficiently large n ,

$$\left\| \Delta_{F_0} \right\|_F = o(n^{1/2}).$$

Proof of Lemma 6. Decompose Δ_{F_0} as

$$\begin{aligned} \Delta_{F_0} &= \left(\hat{V}_0 \hat{V}_0^\top - \bar{V} \bar{V}^\top \right) \left(\frac{1}{m} \sum_k A_k \right) \hat{V}_0 \hat{V}_0^\top + \\ &\quad \dots + \bar{V} \bar{V}^\top \left(\frac{1}{m} \sum_k A_k \right) \left(\hat{V}_0 \hat{V}_0^\top - \bar{V} \bar{V}^\top \right) + \\ &\quad \dots + \bar{V} \bar{V}^\top \left(\frac{1}{m} \sum_k G_k + \frac{1}{m} \sum_k E_k \right) \bar{V} \bar{V}^\top. \end{aligned}$$

Note that for sufficiently large n ,

$$\left\| \frac{1}{m} \sum_k A_k \right\|_2 \leq Cn^\tau,$$

and by triangle inequality and Corollary 5,

$$\|\Delta_{F_0}\|_2 = o(d_1^{-1/2}n^{1/2})$$

which implies $\|\Delta_{F_0}\|_F = o(n^{1/2})$, since $\text{rank}(\Delta_{F_0}) \leq 2d_1$. \square

With control of the error of the initializer $\hat{F}^{(0)}$, Lemma 7 bounds the first-iteration error for each individual matrix G_k using an argument from Koltchinskii et al. [2011].

Lemma 7. For $k = 1, \dots, m$, denote $\Delta_{G_k} = \hat{G}_k - G_k$. Set $\lambda = 3\sigma\sqrt{n}$. Suppose the assumptions of Theorem 1 hold, and \mathcal{E} holds. Then for sufficiently large n , and for all $k = 1, \dots, m$,

$$\|\Delta_{G_k}\|_F \leq C\sigma d_2^{1/2}n^{1/2} \quad (43)$$

for some constant $C > 0$. Moreover, \hat{G}_k is positive semi-definite.

Proof of Lemma 7. Fix $k = 1, \dots, m$. By optimality, there exists some $S_{G_k} \in \partial\|\hat{G}_k\|_*$ such that

$$\langle -(A_k - \hat{F}_0 - \hat{G}_k) + \lambda S_{G_k}, \hat{G}_k - \tilde{G} \rangle \leq 0$$

where \tilde{G} is some matrix with the same support (column space, row space) as G . Let $\tilde{S}_G \in \partial\|\tilde{G}\|_*$ be arbitrary. Adding and subtracting $\lambda\langle \tilde{S}_G, \hat{G}_k - \tilde{G} \rangle$ and $\langle F + G_k, \hat{G}_k - \tilde{G} \rangle$ gives

$$\langle \hat{F}_0 - F + (\hat{G}_k - G_k), \hat{G}_k - \tilde{G} \rangle + \lambda\langle S_{G_k} - \tilde{S}_G, \hat{G}_k - \tilde{G} \rangle \leq \langle -\lambda\tilde{S}_G + E_k, \hat{G}_k - \tilde{G} \rangle. \quad (44)$$

By a convexity argument from Koltchinskii et al. [2011],

$$\langle S_{G_k} - \tilde{S}_G, \hat{G}_k - \tilde{G} \rangle \geq 0. \quad (45)$$

In particular, by convexity of the nuclear norm,

$$\begin{aligned} \|\hat{G}_k\|_* - \|\tilde{G}\|_* &\geq \langle \tilde{S}_G, \hat{G}_k - \tilde{G} \rangle, \\ \|\tilde{G}\|_* - \|\hat{G}_k\|_* &\geq \langle S_{G_k}, \tilde{G} - \hat{G}_k \rangle, \end{aligned}$$

which together establish (45). Furthermore, letting

$$\tilde{S}_G = \sum uv^\top + \mathcal{P}_{G_k}^\perp W \mathcal{P}_{G_k}^\perp,$$

for $\|W\|_2 \leq 1$, we can specify W to maximize

$$\langle \mathcal{P}_{G_k}^\perp W \mathcal{P}_{G_k}^\perp, \hat{G}_k - \tilde{G} \rangle = \langle W, \mathcal{P}_{G_k}^\perp \hat{G}_k \mathcal{P}_{G_k}^\perp \rangle,$$

which by duality of operator and nuclear norm gives maximum value

$$\|\mathcal{P}_{G_k}^\perp \hat{G}_k \mathcal{P}_{G_k}^\perp\|_*.$$

(44) now becomes

$$\langle \hat{G}_k - G_k, \hat{G}_k - \tilde{G} \rangle + \lambda\|\mathcal{P}_{G_k}^\perp \hat{G}_k \mathcal{P}_{G_k}^\perp\|_* \leq \langle -\lambda \sum uv^\top + E_k - \Delta_{F_0}, \hat{G}_k - \tilde{G} \rangle. \quad (46)$$

We bound the first two terms of the RHS of (46) separately. For the first term, by duality

$$|\langle -\lambda \sum uv^\top, \hat{G}_k - \tilde{G} \rangle| \leq \lambda\|\mathcal{P}_{G_k}(\hat{G}_k - \tilde{G})\mathcal{P}_{G_k}\|_* \leq \lambda\sqrt{d_2}\|\hat{G}_k - \tilde{G}\|_F. \quad (47)$$

For the second term,

$$\begin{aligned}
\langle E_k, \hat{G}_k - \tilde{G} \rangle &= \langle E_k - \mathcal{P}_{\tilde{G}_k}^\perp E_k \mathcal{P}_{\tilde{G}_k}^\perp, \hat{G}_k - \tilde{G} \rangle + \langle \mathcal{P}_{\tilde{G}_k}^\perp E_k \mathcal{P}_{\tilde{G}_k}^\perp, \hat{G}_k - \tilde{G} \rangle \\
&\leq \|E_k - \mathcal{P}_{\tilde{G}_k}^\perp E_k \mathcal{P}_{\tilde{G}_k}^\perp\|_F \|\hat{G}_k - \tilde{G}\|_F + \|E_k\|_2 \|\mathcal{P}_{\tilde{G}_k}^\perp \hat{G}_k \mathcal{P}_{\tilde{G}_k}^\perp\|_* \\
&\leq 2\sqrt{d_2} \|E_k\|_2 \|\hat{G}_k - \tilde{G}\|_F + \|E_k\|_2 \|\mathcal{P}_{\tilde{G}_k}^\perp \hat{G}_k \mathcal{P}_{\tilde{G}_k}^\perp\|_*.
\end{aligned}$$

Combining the previous display and (47), and specifying $\tilde{G} = G_k$, we get

$$\begin{aligned}
&\|\Delta_{G_k}\|^2 + (\lambda - \|E_k\|_2) \|\mathcal{P}_{G_k}^\perp \hat{G}_k \mathcal{P}_{G_k}^\perp\|_* \\
&\leq \left(\lambda\sqrt{d_2} + 2\sqrt{d_2} \|E_k\|_2 + \|G_k\|_F \right) \|\Delta_{G_k}\|_F - \langle \Delta_{G_k}, \Delta_{F_0} \rangle.
\end{aligned}$$

Since $\lambda = 3\sigma\sqrt{n} \geq \|E_k\|_2$, the second term on the left-hand side is non-negative, and the first term on the right-hand side can be bounded:

$$\|\Delta_{G_k}\|^2 \leq C\sigma d_2^{1/2} n^{1/2} \|\Delta_{G_k}\|_F - \langle \Delta_{G_k}, \Delta_{F_0} \rangle.$$

Dividing through by $\|\Delta_{G_k}\|_F$, we get

$$\|\Delta_{G_k}\|_F \leq C\sigma d_2^{1/2} n^{1/2} - \langle \Delta_{F_0}, \frac{\Delta_{G_k}}{\|\Delta_{G_k}\|_F} \rangle.$$

Then by trace duality, and since $\|\Delta_{F_0}\|_F = o(n^{1/2})$, for sufficiently large n ,

$$\|\Delta_{G_k}\|_F \leq C\sigma d_2^{1/2} n^{1/2}.$$

for some constant $C > 0$, as desired.

To show \hat{G}_k is positive semi-definite, fix a unit vector $v \in \mathbb{R}^n$. Note that since $\|\Delta_{F_0}\|_2 = o(n^{1/2})$, $\|E_k\|_2 + \|\Delta_{F_0}\|_2 < 3\sigma\sqrt{n} = \lambda$ for sufficiently large n . Then

$$v^\top (G_k + E_k + \Delta_{F_0}) v \geq v^\top (E_k + \Delta_{F_0}) v \geq -(\|E_k\|_2 + \|\Delta_{F_0}\|_2) > -\lambda.$$

Therefore only positive eigenvalues will survive the soft thresholding step

$$\hat{G}_k = S_\lambda(G_k + E_k - \Delta_{F_0}),$$

which completes the proof. \square

In preparation to bound the norm of the sum of errors for all G_k matrices, Lemmas 8 and 9 establish bounds on the recovery of their eigenvectors, and ranks.

Lemma 8. Suppose the assumptions of Theorem 1 hold, and \mathcal{E} holds. For $k = 1, \dots, m$, let \hat{U}_k denote the first d_2 eigenvectors of $G_k + E_k - \Delta_{F_0}$. Then for sufficiently large n , and for constants C and C' ,

$$\inf_{O \in \mathcal{O}_{d_2}} \|\hat{U}_k - \bar{U}_k O\|_2 \leq C\sigma n^{1/2-\tau}, \quad (48)$$

$$\|\hat{U}_k \hat{U}_k^\top - \bar{U}_k \bar{U}_k^\top\|_2 \leq C'\sigma n^{1/2-\tau}. \quad (49)$$

Proof of Lemma 8. By [Cape et al. \[2019\]](#), Theorem 6.9, we have

$$\inf_{O \in \mathcal{O}_{d_2}} \|\hat{U}_k - \bar{U}_k O\|_2 \leq \frac{\|E_k + \Delta_{F_0}\|_2}{b_1 n^\tau}. \quad (50)$$

We also have

$$\|E_k + \Delta_{F_0}\|_2 \leq \|E_k\|_2 + \|\Delta_{F_0}\|_2 \leq C\sigma\sqrt{n}, \quad (51)$$

for some constant C by Lemma 6.

Combining (51) with (50) establishes (48). We also have

$$\|\hat{U}_k \hat{U}_k^\top - \bar{U}_k \bar{U}_k^\top\|_2 = \|\sin \Theta(\hat{U}_k, \bar{U}_k)\|_2,$$

which along with [Cape et al. \[2019\]](#), Theorem 6.9, establishes (49). \square

Lemma 9. Suppose the assumptions of Theorem 1 hold, and \mathcal{E} holds. Then for all $k = 1, \dots, m$, and for sufficiently large n , $\text{rank}(\hat{G}_k) \leq d_2$.

Proof of Lemma 9. Recall that $\hat{G}_k = S_\lambda(G_k + E_k - \Delta_{F_0})$, and \hat{U}_k denotes the first d_2 eigenvectors of $G_k + E_k - \Delta_{F_0}$. Let $v \perp \text{col}(\hat{U}_k)$ be an orthogonal unit vector. Then

$$\|\bar{U}_k^\top v\| \leq \inf_{O \in \mathcal{O}_{d_2}} \|\bar{U}_k^\top v - O \hat{U}_k^\top v\|_2 \leq C\sigma n^{1/2-\tau} \quad (52)$$

by Lemma 8. Further,

$$|v^\top G_k v| = |v^\top \bar{U}_k \bar{U}_k^\top G_k \bar{U}_k \bar{U}_k^\top v| \leq \|G_k\|_2 \left(\inf_{O \in \mathcal{O}_{d_2}} \|\bar{U}_k - \hat{U}_k O\|_2 \right)^2 \leq C\sigma^2 n^{1-\tau}$$

Then

$$|v^\top (G_k + E_k - \Delta_F) v| \leq C\sigma^2 n^{1-\tau} + \|E_k\|_2 + \|\Delta_{F_0}\|_2 \leq \frac{5}{2}\sigma\sqrt{n} \quad (53)$$

for sufficiently large n , since $\tau > 1/2$ and $\|\Delta_{F_0}\|_2 = o(n^{1/2})$. Then since $\lambda = 3\sigma\sqrt{n}$,

$$|\gamma_{d_2+1}(G_k + E_k - \Delta_{F_0})| < \lambda$$

for n sufficiently large, which implies $\text{rank}(\hat{G}_k) \leq d_2$. \square

The next technical lemma will be applied to establish the approximation error of an orthonormal basis to the direct sum of the column spaces the G_k matrices. It follows from basic algebra and is given here without proof.

Lemma 10. Let $v \in \mathbb{R}^n$ be a unit vector, and S be a d -dimensional subspace of \mathbb{R}^n with orthonormal basis $U \in \mathbb{R}^{n \times d}$. Suppose $\|U^\top v\|_2 \leq \epsilon < 1$. Define the orthonormalization of v by

$$\tilde{v} = \frac{\mathcal{P}_S^\perp v}{\|\mathcal{P}_S^\perp v\|_2} = \frac{(I - UU^\top)v}{\|(I - UU^\top)v\|_2}.$$

Then

$$\|v - \tilde{v}\|_2 \leq \frac{2\epsilon}{1 - \epsilon}.$$

As further preparation to bound the norm of the sum of errors for all the G_k matrices, we provide

an orthonormal basis which approximates the column space of each G_k . Lemma 11 establishes a bound on the error of this approximation.

Lemma 11. Suppose the assumptions of Theorem 1 hold. Then there exists a collection mutually orthogonal matrices $\{U_k^*\}_{k=0}^m$ such that U_0^* is an orthonormal basis for $(\text{col}(G_1) + \dots + \text{col}(G_m))^\perp$, and for $k = 1, \dots, m$, U_k^* satisfies

$$\|\bar{U}_k - U_k^*\|_2 \leq C\sigma 2^{d_2/2} m^{1/2} n^{1/2-\tau}.$$

Proof of Lemma 11. Note that the columns of each \bar{U}_k form an orthonormal basis for $\text{col}(G_k)$. Let the columns of L be an orthonormal basis for $(\text{col}(G_1) + \dots + \text{col}(G_m))^\perp$, which is an $n - md_2$ dimensional subspace of \mathbb{R}^n . Then the columns of

$$[\bar{U}_1 \ \bar{U}_2 \ \dots \ \bar{U}_m \ L] \quad (54)$$

form a (non-orthonormal) basis for \mathbb{R}^n . Perform Gram-Schmidt orthonormalization on this matrix from left to right, which will produce a new orthonormal matrix

$$[\bar{U}_1 \ U_2^* \ \dots \ U_m^* \ L]. \quad (55)$$

Note that U_1 and L are left unchanged. Also note that for $2 \leq k \leq m$,

$$\text{col}(\bar{U}_1) + \text{col}(\bar{U}_2) + \dots + \text{col}(\bar{U}_k) = \text{col}(\bar{U}_1) \oplus \text{col}(U_2^*) \oplus \dots \oplus \text{col}(U_k^*).$$

For fixed $k \in \{2, \dots, m\}$, and $j \in \{1, \dots, d_2\}$, consider $u_{k,j}^*$, the j th column of U_k^* and $\bar{u}_{k,j}$, the j th column of \bar{U}_k . By Gram-Schmidt orthonormalization,

$$u_{k,j}^* = \frac{\mathcal{P}_{S_{k,j}}^\perp \bar{u}_{k,j}}{\|\mathcal{P}_{S_{k,j}}^\perp \bar{u}_{k,j}\|_2}$$

where $S_{k,j}$ is the subspace

$$\text{col}(\bar{U}_1) \oplus \text{col}(U_2^*) \oplus \dots \oplus \text{col}(U_{k-1}^*) \oplus \text{col}([u_{k,1}^* \ \dots \ u_{k,j-1}^*]),$$

the span of the previous (orthonormal) columns of (55). Note that when $j = 1$, the final subspace in the direct sum is trivial.

We will use Lemma 10 repeatedly to bound $\|\bar{u}_{k,j} - u_{k,j}^*\|_2$. By construction $\bar{u}_{k,j}$ is a unit vector. An orthonormal basis for $S_{k,j}$ is given by the columns of

$$[\bar{U}_1 \ U_2^* \ \dots \ U_{k-1}^* \ u_{k,1}^* \ \dots \ u_{k,j-1}^*] \in \mathbb{R}^{n \times [(k-1)d_2 + (j-1)]}$$

Then

$$\begin{aligned}
& \|\left[\bar{U}_1 \quad U_2^* \quad \cdots \quad U_{k-1}^* \quad u_{k,1}^* \quad \cdots \quad u_{k,j-1}^*\right]^\top \bar{u}_{k,j}\|_2^2 \\
&= \|\left[\bar{U}_1 \quad U_2^* \quad \cdots \quad U_{k-1}^*\right]^\top \bar{u}_{k,j}\|_2^2 + \sum_{\ell=1}^{j-1} |u_{k,\ell}^{*\top} \bar{u}_{k,j}|^2 \\
&= \|\left[\bar{U}_1 \quad U_2^* \quad \cdots \quad U_{k-1}^*\right]^\top \bar{u}_{k,j}\|_2^2 + \sum_{\ell=1}^{j-1} |(u_{k,\ell}^* - \bar{u}_{k,\ell})^\top \bar{u}_{k,j}|^2 \\
&\leq \|\left[\bar{U}_1 \quad U_2^* \quad \cdots \quad U_{k-1}^*\right]^\top \bar{u}_{k,j}\|_2^2 + \sum_{\ell=1}^{j-1} \|u_{k,\ell}^* - \bar{u}_{k,\ell}\|^2.
\end{aligned} \tag{56}$$

Now (56) and Lemma 10 will be applied inductively for $j = 1, \dots, d_2$.

For $j = 1$, the second sum is empty and by assumption (see (15)),

$$\|\left[\bar{U}_1 \quad U_2^* \quad \cdots \quad U_{k-1}^*\right]^\top \bar{u}_{k,1}\|_2 \leq C\sigma(k-1)^{1/2}n^{-1/2} \leq C\sigma m^{1/2}n^{1/2-\tau}.$$

Then by Lemma 10,

$$\|\bar{u}_{k,1} - u_{k,1}^*\|_2 \leq \frac{2C\sigma m^{1/2}n^{1/2-\tau}}{1 - C\sigma m^{1/2}n^{1/2-\tau}} \leq C\sigma m^{1/2}n^{1/2-\tau}$$

for sufficiently large n , since $mn^{1-2\tau} \rightarrow 0$.

For $j = 2$, we get

$$\|\left[\bar{U}_1 \quad U_2^* \quad \cdots \quad U_{k-1}^* \quad u_{k,1}^*\right]^\top \bar{u}_{k,2}\|_2^2 \leq 2C\sigma^2 mn^{1-2\tau}$$

by (56), the orthogonality assumption, and the $j = 1$ case. Then Lemma 10 gives

$$\|\bar{u}_{k,2} - u_{k,2}^*\|_2 \leq 2C\sigma m^{1/2}n^{1/2-\tau}$$

for sufficiently large n . Continuing for general $j \leq d_2$, the errors compound and we get

$$\|\left[\bar{U}_1 \quad U_2^* \quad \cdots \quad U_{k-1}^* \quad u_{k,1}^* \quad \cdots \quad u_{k,j-1}^*\right]^\top \bar{u}_{k,j}\|_2^2 \leq C\sigma^2 \left(1 + \sum_{\ell=1}^{j-1} 2^{\ell-1}\right) mn^{1-2\tau} \leq C\sigma^2 2^{d_2} mn^{1-2\tau},$$

which gives

$$\|\bar{u}_{k,j} - u_{k,j}^*\|_2 \leq C\sigma 2^{(j-1)/2} m^{1/2} n^{1/2-\tau}$$

for sufficiently large n since $2^{d_2} mn^{1-2\tau} \rightarrow 0$.

We then use each of these to bound the (squared) operator norm for $k = 1, \dots, m$:

$$\begin{aligned}
\|\bar{U}_k - U_k^*\|_2^2 &\leq \|\bar{U}_k - U_k^*\|_F^2 = \sum_{j=1}^{d_2} \|\bar{u}_{k,j} - u_{k,j}^*\|_2^2 \\
&\leq \sum_{j=1}^{d_2} C\sigma^2 2^{j-1} mn^{1-2\tau} \leq C\sigma^2 2^{d_2} mn^{1-2\tau}.
\end{aligned}$$

Thus, the matrix in (55) provides an orthogonal decomposition of \mathbb{R}^n into $m + 1$ pieces, which satisfies

$$\|\bar{U}_k - U_k^*\|_2 \leq C\sigma 2^{d_2/2} m^{1/2} n^{1/2-\tau} \quad (57)$$

for $k \in \{2, \dots, m\}$ and for some constant $C > 0$. For ease of notation we will denote $U_1^* := \bar{U}_1$, and $U_0^* := L$, which both trivially satisfy (57). \square

With Lemmas 8, 9 and 10 in hand, in Lemma 12 we establish a bound on the norm of the sum of the errors for each G_k matrix.

Lemma 12. Suppose the assumptions of Theorem 1 hold, and \mathcal{E} holds. Then for sufficiently large n and some constant C ,

$$\left\| \sum_{k=1}^m \Delta_{G_k} \right\|_2 \leq C\sigma m^{1/2} n^{1/2} \quad (58)$$

Proof of Lemma 12. By (12), for sufficiently large n we have

$$\|\hat{G}_k\|_2 = \|G_k + E_k - \Delta_{F_0}\|_2 - \lambda \leq B_1 n^\tau + \|E_k\|_2 + \|\Delta_{F_0}\|_2 - \lambda \leq Cn^\tau \quad (59)$$

for some constant C , since $\tau > 1/2$.

By Lemma 9, \hat{G}_k satisfies

$$\hat{G}_k = \hat{U}_k \hat{U}_k^\top \hat{G}_k \hat{U}_k \hat{U}_k^\top,$$

for sufficiently large n , and thus Δ_{G_k} admits the decomposition

$$\begin{aligned} & \hat{U}_k \hat{U}_k^\top \hat{G}_k \hat{U}_k \hat{U}_k^\top - \bar{U}_k \bar{U}_k^\top G_k \bar{U}_k \bar{U}_k^\top \\ &= (\hat{U}_k \hat{U}_k^\top - \bar{U}_k \bar{U}_k^\top) \hat{G}_k \hat{U}_k \hat{U}_k^\top + \bar{U}_k \bar{U}_k^\top \Delta_{G_k} \hat{U}_k \hat{U}_k^\top + \bar{U}_k \bar{U}_k^\top G_k (\hat{U}_k \hat{U}_k^\top - \bar{U}_k \bar{U}_k^\top) \\ &=: (\mathcal{I})_k + (\mathcal{II})_k + (\mathcal{III})_k. \end{aligned} \quad (60)$$

We bound the operator norm of each of these three terms separately.

Term (\mathcal{I}) . By Lemma 8, (59), and submultiplicativity,

$$\|(\hat{U}_k \hat{U}_k^\top - \bar{U}_k \bar{U}_k^\top) \hat{G}_k \hat{U}_k \hat{U}_k^\top\|_2 \leq C\sigma n^{1/2} \quad (61)$$

for some constant $C > 0$. We also have, for $k \neq j$ and arbitrary $O_1, O_2 \in \mathcal{O}_{d_2}$,

$$\begin{aligned} \|\hat{U}_k^\top \hat{U}_j\|_2 &= \|\hat{U}_k^\top \hat{U}_j - \hat{U}_k^\top \bar{U}_j O_1 + \hat{U}_k^\top \bar{U}_j O_1 - O_2 \bar{U}_k^\top \bar{U}_j O_1 + O_2 \bar{U}_k^\top \bar{U}_j O_1\|_2 \\ &\leq \|\hat{U}_j - \bar{U}_j O_1\|_2 + \|\hat{U}_k - \bar{U}_k O_2\|_2 + \|\bar{U}_k^\top \bar{U}_j\|_2 \end{aligned}$$

and thus taking infimums over \mathcal{O}_{d_2} , and by Lemma 8,

$$\|\hat{U}_k^\top \hat{U}_j\|_2 \leq C\sigma n^{1/2-\tau} \quad (62)$$

for some constant $C > 0$. It follows that

$$\|(\hat{U}_k \hat{U}_k^\top - \bar{U}_k \bar{U}_k^\top) \hat{G}_k \hat{U}_k \hat{U}_k^\top \hat{U}_j \hat{U}_j^\top \hat{G}_j (\hat{U}_j \hat{U}_j^\top - U_j U_j^\top)\|_2 \leq C(\sigma n^{1/2})^2 \cdot (\sigma n^{1/2-\tau}), \quad (63)$$

so by Lemma 4,

$$\left\| \sum_{k=1}^m (\mathcal{I})_k \right\|_2 \leq C\sigma m^{1/2} n^{1/2} \left(1 + \sigma m n^{1/2-\tau} \right) \leq C\sigma m^{1/2} n^{1/2} \quad (64)$$

for sufficiently large n , by Assumption 1.

Term (\mathcal{II}) . Using the variational definition of the operator norm,

$$\left\| \sum_{k=1}^m (\mathcal{II})_k \right\|_2 = \sup_{x, y \in \mathbb{R}^n} \frac{x^\top \left(\sum_{k=1}^m (\mathcal{II})_k \right) y}{\|x\|_2 \|y\|_2}.$$

Fix vectors $x, y \in \mathbb{R}^n$. By Lemma 11, we can write $x = \sum_{i=0}^m x_i$ where

$$x_i = U_i^* U_i^{\top} x,$$

and $\{U_i^*\}_{i=0}^m$ is a collection of mutually orthogonal matrices, with U_0^* an orthonormal basis for $(\text{col}(G_1) + \dots + \text{col}(G_m))^\perp$. For $k = 1, \dots, m$, U_k^* satisfies

$$\|\bar{U}_k - U_k^*\|_2 \leq C\sigma 2^{d_2/2} m^{1/2} n^{1/2-\tau}.$$

Moreover, $\sum_i \|x_i\|_2^2 = \|x\|_2^2$, and as a result,

$$\sum_i \|x_i\|_2 \leq \sqrt{2m} \|x\|_2. \quad (65)$$

Decompose y similarly, and write

$$\left(\sum_{i=0}^m x_i \right)^\top \left(\sum_{k=1}^m (\mathcal{II})_k \right) \left(\sum_{j=0}^m y_j \right) = \sum_{k=1}^m \sum_{i=0}^m \sum_{j=0}^m x_i^\top \bar{U}_k \bar{U}_k^\top \Delta_{G_k} \hat{U}_k \hat{U}_k^\top y_j. \quad (66)$$

We will bound four types of terms of (66) individually. First, if $i = j = k$, we have

$$|x_k^\top \bar{U}_k \bar{U}_k^\top \Delta_{G_k} \hat{U}_k \hat{U}_k^\top y_k| \leq \|\Delta_{G_k}\|_F \|x_k\|_2 \|y_k\|_2 \leq C\sigma d_2^{1/2} n^{1/2} \|x_k\|_2 \|y_k\|_2, \quad (67)$$

where the final inequality follows from Lemma 7. By Cauchy-Schwarz inequality,

$$\sum_{k=1}^m \|x_k\|_2 \|y_k\|_2 \leq \left(\sum_{k=1}^m \|x_k\|_2^2 \right)^{1/2} \left(\sum_{k=1}^m \|y_k\|_2^2 \right)^{1/2} \leq 1,$$

so the total contribution is bounded by

$$C\sigma d_2^{1/2} n^{1/2}. \quad (68)$$

If $i = k \neq j$, with U_0 as defined above, we have

$$\begin{aligned} |x_k^\top \bar{U}_k \bar{U}_k^\top \Delta_{G_k} \hat{U}_k \hat{U}_k^\top y_j| &= |x_k^\top \bar{U}_k \bar{U}_k^\top \Delta_{G_k} \hat{U}_k \hat{U}_k^\top U_j^* U_j^{\top} y_j| \\ &\leq \|x_k\|_2 \|\Delta_{G_k}\|_F \|\hat{U}_k U_j^*\|_2 \|y_j\|_2 \\ &\leq C\sigma^2 d_2^{1/2} 2^{d_2/2} m^{1/2} n^{1-\tau} \|x_k\|_2 \|y_j\|_2, \end{aligned} \quad (69)$$

where the final inequality uses Lemma 7. To bound $\|\hat{U}_k^\top U_j^*\|_2$, first write

$$\|\hat{U}_k^\top U_j^*\|_2 = \|\hat{U}_k^\top U_j^* - \hat{U}_k^\top U_j + \hat{U}_k^\top U_j\|_2 \leq \|U_j^* - \bar{U}_j\|_2 + \|\hat{U}_k^\top \bar{U}_j\|_2.$$

By Lemma 11, the first term is bounded by

$$C\sigma 2^{d_2/2} m^{1/2} n^{1/2-\tau}.$$

For the second term, note that for any $O \in \mathcal{O}_{d_2}$,

$$\begin{aligned} \|\hat{U}_k^\top \bar{U}_j\|_2 &= \|\hat{U}_k^\top \bar{U}_j - O^\top \bar{U}_k^\top \bar{U}_j + O^\top \bar{U}_k^\top \bar{U}_j\|_2 \\ &\leq \|\hat{U}_k^\top - (\bar{U}_k O)^\top\|_2 \|\bar{U}_j\|_2 + \|O^\top\|_2 \|\bar{U}_k^\top \bar{U}_j\|_2. \end{aligned}$$

Taking an infimum over O and applying Assumption 2, Lemma 8 and the fact that $\bar{U}_k^\top U_0^* = 0$ for $k = 1, \dots, m$, we get that

$$\|\hat{U}_k^\top \bar{U}_j\|_2 \leq C\sigma n^{1/2-\tau}.$$

Summing over the terms in (69), the total contribution is then bounded by

$$C\sigma^2 d_2^{1/2} 2^{d_2/2} m^{3/2} n^{1-\tau}. \quad (70)$$

If $i \neq k = j$, the total contribution can be similarly bounded. Finally, if $i \neq k \neq j$,

$$\begin{aligned} |x_i^\top \bar{U}_k \bar{U}_k^\top \Delta_{G_k} \hat{U}_k \hat{U}_k^\top y_j| &= |x_i^\top U_i^* U_i^{*\top} \bar{U}_k \bar{U}_k^\top \Delta_{G_k} \hat{U}_k \hat{U}_k^\top U_j^* U_j^{*\top} y_j| \\ &\leq \|x_i\|_2 \|U_i^{*\top} \bar{U}_k\|_2 \|\Delta_{G_k}\|_F \|\hat{U}_k U_j^*\|_2 \|y_j\|_2 \leq C\sigma^3 d_2^{1/2} 2^{d_2} m n^{3/2-2\tau} \|x_i\|_2 \|y_j\|_2. \end{aligned}$$

The total contribution can be bounded above by

$$C\sigma^3 d_2^{1/2} 2^{d_2} m^3 n^{3/2-2\tau}. \quad (71)$$

Combining (68)-(71), we get the upper bound

$$\frac{x^\top (\sum_{k=1}^m (\mathcal{II})_k) y}{\|x\|_2 \|y\|_2} \leq C\sigma n^{1/2} d_2^{1/2} \left(1 + \sigma 2^{d_2/2} m^{3/2} n^{1/2-\tau} + \sigma^2 2^{d_2} m^3 n^{1-2\tau}\right),$$

and thus

$$\left\| \sum_{k=1}^m (\mathcal{II})_k \right\|_2 \leq C\sigma m^{1/2} n^{1/2} \quad (72)$$

for sufficiently large n , by Assumption 1.

Term (\mathcal{III}) . The proof proceeds similarly to term (\mathcal{I}) , resulting in, for sufficiently large n ,

$$\left\| \sum_{k=1}^m (\mathcal{III})_k \right\|_2 \leq C\sigma m^{1/2} n^{1/2}. \quad (73)$$

Combining (64), (72), and (73),

$$\left\| \sum_{k=1}^m \Delta_{G_k} \right\|_2 \leq C\sigma m^{1/2} n^{1/2} \quad (74)$$

for sufficiently large n . □

The next two lemmas apply Lemma 12 to establish that the first-iteration estimator of F is low-rank. The proofs of Lemma 13 and Lemma 14 take approaches analogous to the proofs of Lemma 8 and

Lemma 9 respectively, and are omitted.

Lemma 13. Suppose the assumptions of Theorem 1 hold, and \mathcal{E} holds. Let \hat{V} denote the first d_1 eigenvectors of $F + \frac{1}{m} \sum_k E_k - \frac{1}{m} \sum_k \Delta_{G_k}$. Then for sufficiently large n and some constant C ,

$$\inf_{O \in \mathcal{O}_{d_1}} \|\hat{V} - \bar{V}O\|_2 \leq C\sigma m^{-1/2} n^{1/2-\tau}. \quad (75)$$

Lemma 14. Suppose the assumptions of Theorem 1 hold, and \mathcal{E} holds. Then $\text{rank}(\hat{F}) \leq d_1$ for sufficiently large n .

To complete the proof of Theorem 1, Lemma 15 applies the same argument from Koltchinskii et al. [2011], as well as Lemmas 12 and 14 to bound the first-iteration error for F .

Lemma 15. Let $\Delta_F = \hat{F} - F$. Suppose the assumptions of Theorem 1 hold, and \mathcal{E} holds. Then for sufficiently large n ,

$$\|\Delta_F\|_F \leq C\sigma d_1^{1/2} m^{-1/2} n^{1/2}$$

for some constant $C > 0$. Moreover, \hat{F} is positive semi-definite.

Proof of Lemma 15. By the same convexity argument as in Lemma 7, we have

$$\begin{aligned} \|\Delta_F\|_F &\leq C\sigma d_1^{1/2} m^{-1/2} n^{1/2} - \frac{1}{m} \sum_k \langle \Delta_{G_k}, \frac{\Delta_F}{\|\Delta_F\|_F} \rangle \\ &\leq C\sigma d_1^{1/2} m^{-1/2} n^{1/2} - \frac{d_1^{1/2}}{m} \sum_k \langle \Delta_{G_k}, \frac{\Delta_F}{\|\Delta_F\|_*} \rangle, \end{aligned}$$

where the second inequality follows by Lemma 14, as long as c_α is sufficiently large. Then by trace duality and Lemma 12,

$$\|\Delta_F\|_F \leq C\sigma d_1^{1/2} m^{-1/2} n^{1/2} + \frac{d_1^{1/2}}{m} \left\| \sum_k \Delta_{G_k} \right\|_2 \leq C\sigma d_1^{1/2} m^{-1/2} n^{1/2}$$

for sufficiently large n , as desired. The argument that \hat{F} is positive semi-definite is analogous to the argument for \hat{G}_k and is omitted. \square

B.3 Proof of Theorem 2

Structurally, the proof of Theorem 2 proceeds similarly to the proof of Theorem 1. The conclusion of the required auxilliary results hold under the assumptions of Theorem 2, with the exception of Lemma 15. In this case, we replace the application of Lemma 12 in the proof of Lemma 15 with the following Lemma 16, which gives the desired conclusion of Theorem 2.

Lemma 16. Suppose the assumptions of Theorem 2 hold, and \mathcal{E} holds. Then for sufficiently large n and some constant C ,

$$\left\| \sum_{k=1}^m \Delta_{G_k} \right\|_2 \leq C\sigma d_2^{1/2} m^{1/2} n^{1/2}.$$

Proof. The proof proceeds similarly to the proof of Lemma 12, beginning with the same decomposition

$$\Delta_{G_k} = (\mathcal{I})_k + (\mathcal{II})_k + (\mathcal{III})_k.$$

We can bound the contribution of (\mathcal{I}) and (\mathcal{III}) by $Cm^{1/2}n^{1/2}$ by the same approach as Lemma 12. We now bound (\mathcal{II}) using Lemma 4, and get

$$\left\| \sum_{k=1}^m (\mathcal{II})_k \right\|_2 \leq C\sigma d_2^{1/2} m^{1/2} n^{1/2}$$

for some constant C and n sufficiently large, completing the proof. \square

B.4 Proof of Proposition 2

Proof of Proposition 2. We prove (21); the proof of (22) is analogous. Let $M^{(j)}$ denote the j th column of a matrix M . Recall that $F = VV^\top$, so the SVD of V can be written as $V = \bar{V}\Gamma_F^{1/2}W^\top$ for some orthonormal matrix $W \in \mathcal{O}_{d_1}$.

Suppose n is sufficiently large so that the conclusions of Theorem 1 hold, and the event \mathcal{E} holds. Denote the truncated eigendecomposition (up to rank d_1) of \hat{F} by

$$\hat{F} = \hat{V}\hat{\Gamma}_F\hat{V}^\top.$$

Then, since \hat{F} is positive semi-semidefinite, the ASE of \hat{F} is given by

$$\hat{V} = \hat{V}\hat{\Gamma}_F^{1/2}.$$

For each $j = 1, \dots, d_1$, choose

$$o_j^* = \operatorname{argmin}_{s \in \{-1, 1\}} \|\hat{V}^{(j)} - s\bar{V}^{(j)}\|_2,$$

and denote $o^* = (o_1^*, \dots, o_{d_1}^*)^\top$. Then

$$\begin{aligned} & \|\hat{V}^{(j)} - o_j^* \bar{V}^{(j)} \gamma_j(F)^{1/2}\|_2 \\ &= \|\hat{V}^{(j)} \gamma_j(\hat{F})^{1/2} - \hat{V}^{(j)} \gamma_j(F)^{1/2} + \hat{V}^{(j)} \gamma_j(F)^{1/2} - o_j^* \bar{V}^{(j)} \gamma_j(F)^{1/2}\|_2 \\ &\leq |\gamma_j(\hat{F})^{1/2} - \gamma_j(F)^{1/2}| + |\gamma_j(F)^{1/2}| \|\hat{V}^{(j)} - o_j^* \bar{V}^{(j)}\|_2 \\ &\leq \frac{|\gamma_j(\hat{F}) - \gamma_j(F)|}{\gamma_j(\hat{F})^{1/2} + \gamma_j(F)^{1/2}} + |\gamma_j(F)^{1/2}| \|\hat{V}^{(j)} - o_j^* \bar{V}^{(j)}\|_2 \\ &\leq C \left(n^{-\tau/2} \left(\sigma d_1^{1/2} m^{-1/2} n^{1/2} \right) + n^{\tau/2} \left(\sigma d_1^{1/2} m^{-1/2} n^{1/2-\xi} \right) \right) \\ &\leq C \sigma d_1^{1/2} m^{-1/2} n^{(1+\tau)/2-\xi} \end{aligned}$$

for sufficiently large n , where in the second-to-last expression, the order of the first term follows by Weyl's inequality [Bhatia, 2013] and Theorem 1, and the order of the second term follows by Cape et al. [2019], Theorem 6.9 along with Theorem 1 and Assumption 4.

Now denote $O^* = W \cdot \operatorname{diag}(o^*) \in \mathcal{O}_{d_1}$, where $\operatorname{diag} : \mathbb{R}^r \rightarrow \mathbb{R}^{r \times r}$ creates a diagonal matrix with

the entries of the vector along the main diagonal. Then

$$\begin{aligned} \inf_{O \in \mathcal{O}_{d_1}} \|\hat{V} - VO\|_F^2 &\leq \|\hat{V} - VO^*\|_F^2 \leq \|\hat{V} - \bar{V}\Gamma_F^{1/2} \text{diag}(o^*)\|_F^2 \\ &= \sum_{j=1}^{d_1} \|\hat{V}^{(j)} - o_j^* \bar{V}^{(j)} \gamma_j(F)\|_2^2 \leq C\sigma^2 d_1^2 m^{-1} n^{1+\tau-2\xi} \end{aligned}$$

which is equivalent to (21). □